

## CHAPTER 4

**STRUCTURAL AND TECHNOLOGICAL SOLUTIONS FOR  
FILM SOLAR CELLS BASED ON CDS/CdTe FOR RESERVE  
POWER SUPPLY OF EMERGENCY PREVENTION SYSTEMS****ABSTRACT**

Investigations of solar cells based on CdS/CdTe, designed for reserve power supply of security systems and control of objects in conditions of damage to the power supply system, have been carried out. An analysis is made of losses in the initial parameters of solar cells based on cadmium telluride, which are due to the design features of the device structure and photoelectric processes occurring in their volume upon absorption of light. Implemented approaches to increasing the efficiency of a photocell based on CdS/CdTe and their effectiveness are studied. Ways are proposed to increase the efficiency of such film solar cells by improving the method of obtaining a rear contact. Design and technological solutions for SC ITO/CdS/CdTe/Cu/Au have been developed, which make it possible to obtain laboratory samples with an efficiency factor of more than 10 %. Laboratory samples of ITO/CdS/CdTe/Cu/ITO CEs have been fabricated, the two-sided illumination of which makes it possible to increase the electric power by 30 %. The research of Cu/ITO transparent rear contacts for CdTe-based solar cells intended for use in tandem and bilaterally sensitive device structures have been studied. The study of the light Current-voltage characteristics of  $\text{SnO}_2\text{:F/CdS/CdTe/Cu/ITO}$  solar cells under illumination from both sides made it possible to establish significant differences in the initial parameters and light diode characteristics under illumination from the side of the glass substrate and from the side of the transparent rear electrode. Testing of laboratory samples of ITO/CdS/CdTe/Cu/ITO solar cells as part of tandem photovoltaic converters has been carried out. Research has been carried out on methods for obtaining CdTe base layers for creating efficient solar cells on a flexible substrate. With a series connection of ITO/CdS/CdTe/Cu/Au SC, experimental samples of micromodules with an efficiency of 5.4 % have been obtained.

**KEYWORDS**

Film solar cell, cadmium telluride, rear contact, transparent rear contact, tandem structure, two-sided sensitive solar cell, flexible substrate, micromodule.

An analysis of emergency situations shows that one of the problems of localization and elimination of consequences is power outages due to damage to power lines. Therefore, it is necessary to provide emergency power supplies or the tools used must work autonomously.

Modern security and control systems consume only a small part of the total energy consumption of the facility, their uninterrupted operation is ensured by the presence of electricity in the network. As a rule, such security systems have a backup power source in case of an emergency power outage in the network, but in most cases, its charge lasts no more than 24 hours. In this case, the use of solar cells becomes relevant. In general, the scope of solar panels is expanding every day. Sometimes the most unexpected branches of industry and the national economy turn to solar cells for help [1–3]. Solar cells are out of competition in places where there is no conventional power grid, but there is enough sun, or in the event of long-term damage to the grid supply of electricity.

Photovoltaic technology is one of the most important renewable energy sources, for which, since its first recognition in 1839, many studies have been carried out to improve their efficiency. But improving the efficiency and reducing the cost of photovoltaic technology still requires a lot of effort. Crystalline silicon (c-Si) solar cells are known as materials in first generation solar cells. In terms of cost, performance and manufacturability, the application of new advanced materials such as amorphous silicon (a-Si), cadmium telluride (CdTe) and indium gallium copper diselenide (CIGS) is achieved in the second and third generations of solar cells. The typical conversion efficiency of first generation technologies is currently between 15 % and 24 %, while that of second generation technologies is currently between 7 % and 16 %. The unique physical characteristics of CdTe make it possible to use the material to create a number of microelectronic devices. Cadmium chalcogenide films are increasingly being used as the base layers of various devices. The main goal of many scientific studies of cadmium telluride should be considered the development of a technology for obtaining thin films of the compound with certain electrical parameters.

Therefore, an urgent topic is the development of approaches to the use of CdTe-based photovoltaic cells for redundant security and control systems in the event of a long-term power outage from utility networks.

## 4.1 STUDY OF FILM SOLAR CELLS BASED ON CDS/CDTE

### 4.1.1 IMPROVING THE EFFICIENCY OF FILM SOLAR CELLS BASED ON CDS/CDTE

Solar cells based on crystalline silicon and thin films are the most common commercial technologies in the field of photovoltaics. However, the dominant position in the market is occupied by solar cells based on crystalline silicon, the serial production of which is 85 % of the world production of all photovoltaic converters [4]. In the manufacture of this type of SC, high-quality raw materials are used, the production of which is currently energy-intensive. In addition, SC based on single-crystal

and polycrystalline silicon are indirect-gap conductors and, accordingly, have a low absorption coefficient. Therefore, for the effective use of solar radiation, the thickness of the base layers should not be less than 200 microns. Also, in such device structures, a significant decrease in efficiency with increasing temperature is observed.

Promising technologies for terrestrial application are solar cells based on CdTe [5].

The formation of such instrumental structures is carried out with less energy consumption for their manufacture. In addition, the technology for producing CdS/CdTe films is rapidly reproducible and makes it possible to form uniform thin films with an area of more than 1 m<sup>2</sup>, which have the highest theoretical efficiency among single-junction photovoltaic converters, 29 % [6]. However, the maximum experimental efficiency is 16.5 % and was recorded for SC based on the CdS/CdTe heterosystem when implementing the back-barrier structure of the devices [7], shown in **Fig. 4.1**.

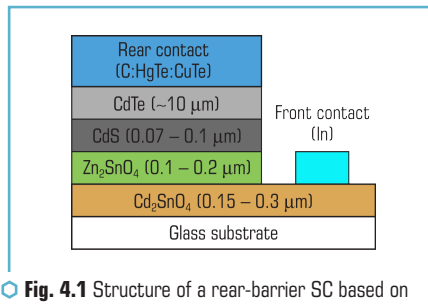


**Fig. 4.1** Structure of a rear-barrier SC based on CdS/CdTe with an efficiency of ~16.5 %

To achieve such high values of the efficiency of creation, shown in **Fig. 4.1**, SC was carried out on borosilicate glass [7], which is more valuable than traditional SiO<sub>2</sub>. The TCO (In<sub>2</sub>O<sub>3</sub>SnO<sub>2</sub>) layer was replaced with a TCO (Cd<sub>2</sub>SnO) layer [7] because the leading oxide Cd<sub>2</sub>SnO<sub>4</sub> has a better combination of optical and electrical properties and has a higher transparency (over 90 %). Thin CdS films were deposited using an aqueous solution of Cd(C<sub>2</sub>H<sub>3</sub>O<sub>2</sub>)<sub>2</sub>, C<sub>2</sub>H<sub>3</sub>O<sub>2</sub>NH<sub>4</sub>, CS(NH<sub>2</sub>)<sub>2</sub>, NH<sub>4</sub>OH and according to the technology described in [8]. The deposition of CdTe was carried out by sublimation in a closed space. After CdTe deposition, the samples were subjected to chloride treatment, which is a mandatory procedure for the formation of efficient CdTe-based SCs [9, 10]. Without chloride treatment, the efficiency of CdTe-based SC is typically <5 %. The chloride treatment is believed to increase the grain size of CdTe, passivate their grain boundaries, and promote efficient adhesion of CdS and CdTe. To form a rear contact, HgTe:CuTe graphite paste was applied, followed by the deposition of silver paste and an antireflection MgF<sub>2</sub> layer.

However, despite the implemented technologies, the efficiency of the obtained samples is far from the theoretical value. Since the formation of stable low-resistance rear contacts is another important step in the fabrication of high-performance CEs based on CdTe/CdS [11].

The main technological approach implemented by many authors when creating low-resistance contacts to SCs based on CdS/CdTe is the formation of tunnel contacts [12]. The formation of an ohmic contact to the p-CdTe base layer under industrial production conditions is not economical, since only platinum has the electron work function necessary for the formation of an ohmic transition. Therefore, tunneling contacts are traditionally formed to p-CdTe layers using thin films containing copper or copper chalcogenide [12]. However, the diffusion of copper into the base layer leads to degradation of the initial parameters of film CEs based on CdS/CdTe. Therefore, comprehensive studies are needed to develop rear contacts in CdTe base layers to create highly efficient, degradation-resistant solar cells.

#### 4.1.2 ANALYSIS OF LOSSES IN THE INITIAL PARAMETERS OF SOLAR CELLS BASED ON CDS/CDTE

The main characteristic of any solar cell is the coefficient of performance (COP). The value of the efficiency of any solar cell is calculated by the formula [13]:

$$\eta = \left( P_{HM} / P_u \right) \times 100 \% = \left[ P_{HM} / \left( P_{r^*} S_{ce} \right) \right] \times 100 \% \quad (4.1)$$

where  $P_{r^*}$  – the specific radiation power on the photoreceiving surface of the solar cell;  $S_{ce}$  – the area of the photoreceiving surface of the solar cell.

The power  $P_{HM}$  depends on three experimentally determined initial parameters of the SC as follows:

$$P_{HM} = I_{sc} V_{nl} FF, \quad (4.2)$$

where  $I_{sc}$  – the short-circuit current;  $V_{nl}$  – the no-load voltage;  $FF$  – the filling factor of the light current-voltage characteristic.

Therefore, to calculate the efficiency of a photoelectric converter, along with formula (4.1), the following relation is used:

$$\eta = \left[ I_{sc} V_{nl} FF / \left( P_{r^*} S_{ce} \right) \right] \times 100 \% \quad (4.3)$$

As can be seen from expression (4.3), the efficiency increases with an increase in each of the three key initial SC parameters –  $I_{sc}$ ,  $V_{nl}$  and  $FF$ , and therefore it is necessary to analyze the losses of these quantities.

Short-circuit current density losses ( $J_{sc}$ ) in the SC are due to the following processes:

- reflection of solar radiation from the surface of the instrumental structure;
- absorption of solar radiation in photoelectrically inactive layers;
- absorption of light in the area of contacts.

The short circuit current density is determined by the following analytical expression:

$$J_{sc} = \int_{\lambda_{min}}^{\lambda_{max}} Q_E(\lambda) J_{sol}(\lambda) d\lambda, \quad (4.4)$$

where  $Q_E(\lambda)$  – the quantum efficiency coefficient,  $J_{sol}$  – the intensity of solar radiation. The losses corresponding to each of the actions described above can be calculated using the following expression:

$$J_{loss} = \int_{\lambda_{min}}^{\lambda_{max}} F(\lambda) J_{sol} d\lambda, \quad (4.5)$$

where  $F(\lambda)$  – the partial reflection or absorption of each wavelength.

The sum of losses and quantum efficiency ( $Q_E$ ) values should be equal to units for all wavelengths.

The main physical mechanisms that cause losses in the value of the open-circuit voltage have not been sufficiently studied at present. It is believed that  $V_{nl}$  is limited by the dominant current flow mechanism. The current-voltage characteristics of a typical solar cell is described as follows [13]:

$$J \approx J_0 \exp \left[ \frac{q(V - V_{p-n})}{AkT} \right] - J_p, \quad (4.6)$$

where  $J_p$  – the photocurrent density;  $J_0$  – the saturation diode current density;  $V$  – the voltage drop across the SC;  $V_{p-n}$  – the potential barrier height;  $q$  – the electron charge;  $k$  – the Boltzmann constant;  $T$  – the temperature of the solar cell;  $A$  – the diode ideality factor. Saturation diode current density ( $J_0$ ) depends on the specific operating mechanism that dominates the forward current flow. Let's assume that the processes in CdTe solar cells are mainly controlled by volume recombination and, therefore,  $J_0$  can be expressed as:

$$J_0 = qp v_r, \quad (4.7)$$

where  $p$  – the hole concentration;  $v_r$  – the recombination rate. Thus,  $V_{nl}$  can be represented as:

$$V_{nl} = V_{p-n} - \frac{AkT}{q} \ln \left( \frac{qp v_r}{J_p} \right). \quad (4.8)$$

The expression relating the height of the potential barrier and the band gap ( $E_g$ ) looks like this:

$$V_{p-n} = \frac{E_g}{q} - \frac{kT}{q} \ln \left( \frac{N_v}{p} \right), \quad (4.9)$$

where  $N_v$  – the effective density of states in the valence band.

So for  $A=2$ :

$$V_{nl} = \frac{E_g}{q} - \frac{kT}{q} \ln \left( \frac{q^2 N_v \rho v_r^2}{J_p^2} \right). \quad (4.10)$$

Regardless of the details,  $V_{nl}$  decreases with increasing recombination rate. Thus, a decrease in recombination should contribute to an increase in  $V_{nl}$ . The ratio of recombination rate to thermal rate is expressed as  $(v_r/v_t)$ , where  $v_t$  is 107 cm/s, and is used as the primary recombination parameter for voltage loss analysis.

To analyze the losses in the value of the replenishment factor of the light current-voltage characteristic ( $FF$ ), an empirical expression is used that determines the dependence of  $FF$  on the open-circuit voltage ( $V_{nl}$ ), diode ideality factor ( $A$ ), series resistance ( $R_s$ ) and shunt conductivity ( $G$ ).

In the absence of series resistance and shunt conductance, the expression for  $FF$  can be represented as [14]:

$$FF_0 = \frac{v_{nl} - \ln(v_{nl} + 0.72)}{v_{nl} + 1}, \quad (4.11)$$

where

$$v_{nl} = \frac{qV_{nl}}{AKT}. \quad (4.12)$$

In the presence of a series resistance ( $R_s$ ), the expression for the filling factor of the light current-voltage characteristic ( $FF_s$ ) becomes:

$$FF_s = FF_0 (1 - R_s / R_E), \quad (4.13)$$

where  $R_x = V_{nl} / J_{sc}$  – characteristic impedance. When the series resistance ( $R_s$ ) and shunt conductance ( $G$ ) are significant, the expression for the duty factor of the light current-voltage characteristic ( $FF_{s+w}$ ) is:

$$FF_{s+w} = FF_s \left[ 1 - \frac{(v_{nl} + 0.72) FF_s}{v_{nl} / (R_E G)} \right]. \quad (4.14)$$

According to expression (4.14), it is obvious that an increase in the value of  $FF_{s+w}$  will contribute to a decrease in  $R_s$  and  $G$ .

### 4.1.3 ANALYSIS OF IMPLEMENTED APPROACHES TO REDUCE LOSSES IN THE INITIAL PARAMETERS OF A SOLAR CELL BASED ON CDS/CDTE

To reduce the reflection of solar radiation from the surface of the device structure, in the design of modern CdS/CdTe film SCs, SnO<sub>2</sub> layers are usually used, which, with a surface resistance of about 10 Ohm/□, have a transmittance of 80 %. An alternative to the traditional SnO<sub>2</sub> layer was the use of Cd<sub>2</sub>SnO<sub>4</sub> oxide as a front, transparent electrode, which has the best combination of optical and electrical properties. Cd<sub>2</sub>SnO<sub>4</sub> layers have a higher transparency (over 90 %), which is achieved by reducing their thickness to 0.1 μm, since their surface resistance is about 3 Ohm/□, which is several times lower than that of traditional SnO<sub>2</sub> electrodes [15–17]. Thus, the use of Cd<sub>2</sub>SnO<sub>4</sub> contributes to the reduction of losses  $J_{sc}$  to the level of 0.62 mA/cm<sup>2</sup> due to absorption in the spectral range (300–800) nm, while for traditional SnO<sub>2</sub> layers such losses are (2.8–1.3) mA/cm<sup>2</sup> [18].

The recombination of nonequilibrium charge carriers generated under the action of photons in the spectral range (300–520) nm in the CdS layer also has a significant negative effect on the  $J_{sc}$  value. Reducing the recombination level can be achieved by reducing the thickness of the CdS layer, however, this leads to a decrease in the values of  $V_{nl}$  and  $FF$ . In [19], it was proposed to use a ZTO buffer layer, which ensures mutual diffusion with the CdS layer during structure formation. During interdiffusion, which occurs at an annealing temperature of 600 °C in the presence of Ar or He, penetration of approximately 3–5 % Cd in the ZTO layer and approximately 2–3 % Zn in the CdS layer is observed. Diffusion at a lower annealing temperature of 420 °C for 15 minutes in the presence of CdCl<sub>2</sub> also indicates a significant amount of abundant Cd and Zn in the ZTO and CdS layers, respectively.

Thus, the consumption of the CdS layer during interdiffusion contributes to a decrease in the absorption of photons with energies exceeding the band gap of CdS, an increase in the quantum efficiency of > 75 % for photons with a wavelength of more than 400 nm, and a decrease in losses  $J_{sc}$  due to absorption 1.0–1.3 mA/cm<sup>2</sup> in the layer, while maintaining high  $V_{nl}$  and  $FF$  values. At present, an obligatory technological operation in the manufacture of high-efficiency film solar cells based on CdS/CdTe is chloride heat treatment [20]. The processes occurring as a result of Cd-Te-CdCl<sub>2</sub> interfacial interaction cause an increase in the grain size of cadmium telluride and cadmium sulfide, as well as an increase in the lifetime of nonequilibrium charge carriers [21]. However, the stresses at the TCO/CdS interface arising as a result of grain growth can significantly impair the adhesion of these layers and contribute to the formation of a bulge. The use of a buffer layer ZTO (Zn<sub>2</sub>SnO<sub>4</sub>) reduces the stress that has arisen in the crystal lattice, providing better adhesion [22]. The use of optimal "chloride" heat treatment and the use of the ZTO buffer layer makes it possible to reduce the diode saturation current density  $J_0$  to 10–11–10<sup>-9</sup> /cm<sup>2</sup> and the diode ideality factor  $A$  to 1.6–2, while for traditional film solar cells based on CdS/CdTe  $J_0 > 10^{-9}$  and  $A > 2$ . The application of this approach makes it possible to reduce losses  $J_{sc}$  due to recombination within grains. There are two theoretical approaches to increase open circuit voltage. The first approach is to increase the concentration of holes (acceptors) in the CdTe layer up to  $2 \times 10^{17}$  cm<sup>-3</sup>. It should be

noted that at present, for a typical SC based on CdTe, the concentration of acceptors in the base layer is three orders of magnitude lower,  $2 \times 10^{14} \text{ cm}^{-3}$ . In this case, a decrease in the width of the depletion region at an increased concentration of charge carriers contributes to an increase in the diffusion length of minority charge carriers, and, therefore, provides an increase in the lifetime, which will increase  $V_{sc}$ . In addition, an increase in the concentration of charge carriers leads to an increase in the height of the potential barrier, the value of which limits the maximum possible value of the open circuit voltage. However, with an increase in the charge carrier concentration, the rate of surface recombination at the CdS/CdTe heterojunction can limit the increase in open circuit voltages due to the intensification of the removal of nonequilibrium charge carriers generated under the action of light in the base layer. In addition, it is impossible to actually achieve the required charge carrier concentrations with existing approaches to reducing resistivity. At present, the decrease in resistivity is carried out with the "chloride" treatment, as a result of which shallow acceptor levels are generated that have defective ClTe – VCd complexes. With an increase in the chlorine concentration, the energy structure of the base layer evolves; as a result of an increase in the concentration, there are no defective complexes described above, but isoelectronic traps 2ClTe – VCd are formed, which contribute to an increase in the resistivity of the base layer [23]. The second approach is to form a p–i–n structure with a hole concentration in the CdTe layer of  $2 \times 10^{13}$ . In this case, the internal field propagates over the entire thickness of CdTe, and the resulting barrier, which is called the "electronic reflector", limits the recombination rate on the rear surface. Without an increase in the conduction band barrier, the voltage is lower than the voltage at a typical charge carrier concentration of  $2 \times 10^{14} \text{ cm}^{-3}$  in CdTe, but even with a modest electronic reflector (0.2 eV), the  $V_{sc}$  voltage should increase significantly. One possibility to create such a barrier is to add a layer of ZnTe [13] or other material with an extended discontinuity in the conduction band. A potential difficulty, however, is that any recombination in CdTe/ZnTe or contact with a reflector is fraught with the positive effect of an "electronic" reflector [24].

To increase the filling factor of the light current-voltage characteristics ( $FF$ ), it is necessary to provide a decrease in  $R_s$  and an increase in  $R_w$ . One way to reduce  $R_s$  is to replace the traditional doped  $\text{SnO}_2$  layer with a  $\text{Cd}_2\text{SnO}_4$  layer, which has a lower resistivity value caused by a high mobility value ( $\mu = 54.5 \text{ cm}^2/(\text{Vs})$ ) and a high level of charge carrier concentration  $n = 8, 94 \times 10^{20} \text{ cm}^{-3}$  while maintaining its transparency, which is twice as much as in the  $\text{SnO}_2$  layer.

An increase in  $R_w$  can be realized by introducing an undoped ZTO ( $\text{Zn}_2\text{SnO}_4$ ) layer about 0.1–0.2  $\mu\text{m}$  thick into the TCO/CdS contact region. With a decrease in the thickness of the CdS layer in order to increase  $J_{sc}$ , small windows appear in it, through which the TCO contacts p-CdTe and the p-n junction is shunted. A high-resistance ZTO layer with an optical band gap ( $\sim 3.6 \text{ eV}$ ) prevents the appearance of a defective TCO/CdTe heterojunction. By implementing the approaches described above, the authors of [25] managed to increase the  $FF$  value to the level of 77.34 %.

The analysis performed shows that many directions for increasing the efficiency of SCs based on cadmium telluride have already been practically implemented. At the same time, insufficient attention is currently paid to the problems of increasing the efficiency by optimizing the rear contacts.

#### 4.1.4 FORMATION OF LOW-RESISTANCE REAR CONTACTS IN SC BASE LAYERS BASED ON CDS/CDTE

The efficiency of operation, as well as the resistance to degradation of SC based on CdS/CdTe, depends on the material and method of obtaining the rear contact. When a metal film is deposited on the surface of the CdTe layer, a Schottky barrier is formed. Because the electronic affinity of CdTe is so great, only metals with a work function  $>5.7$  eV form ohmic contacts. Platinum has the highest work function (5.5 eV). But such a material is not economically feasible to use [25].

Therefore, a tunnel junction is usually used as a rear contact. To do this, CdTe is digested on the back surface to form an excess of elemental Te [26]. The next step is to deposit CdTe or a semimetal with a low bandgap on the surface of a semiconductor in the form of a thin buffer layer ( $\sim 10$  nm), followed by the deposition of a metallization layer.

Base film CdS/CdTe heterosystems were deposited by thermal vacuum evaporation in a single technological cycle. The formation of film back contacts, which are Cu/Au film heterostructures of nanosized thickness, was also carried out by this method. The back contacts of the ITO films (indium and tin oxides) were deposited by non-reactive DC magnetron sputtering using an original material-saving magnetron. Before applying the rear contacts, the cadmium telluride surface was etched in a 5% solution of bromine in methanol for 10 seconds. Then, copper layers 12 nm thick and a gold film 50 nm thick were deposited on the surface of the base layer by thermal condensation without heating the substrate. After that, annealing was carried out in air at a temperature of 200 °C for 30 minutes. In this case, during the previous 10 minutes, the laboratory sample was heated up to annealing. In addition to laboratory samples with standard technological operations during the formation of rear contacts, let's analyze SCs in the design of the rear contacts of which there was no copper layer and which, after obtaining the Cu/Au film heterosystem, were not annealed.

To study the effect of a nanosized copper layer in the back contact design on the efficiency of photovoltaic processes in ITO/CdS/CdTe film SCs, let's measure the light current-voltage characteristics of a series of samples with different back contact design solutions at an illumination power of 10 mW/cm<sup>2</sup> to 10 (100 mW/cm<sup>2</sup> corresponds to the standard mode lighting AM1) [27].

Thus, in the process of studying SCs based on CdS/CdTe with a back contact consisting of a copper interlayer 12 nm thick and a layer of gold 50 nm thick, as well as SCs whose back contact does not include copper, it was found that the SC efficiency at power illumination of 1000 W/m<sup>2</sup> with the Cu/Au rear contact approaches 10%, and with the Au rear contact it approaches 3.1%, which is primarily due to the high value of the open circuit voltage and the filling factor of the light CVC. The dependence of the short circuit current density on the level of illumination of both types of contacts is traditionally linear (**Fig. 4.2, a**). In this case, for a SC with a rear contact containing copper, at a radiation power of 70 mW/cm<sup>2</sup>, the maximum efficiency is observed, and for device structures with a rear contact of Au, the efficiency somewhat increases with increasing illumination. The light current-voltage characteristics of the SC at different illumination powers are shown in **Fig. 4.2**.

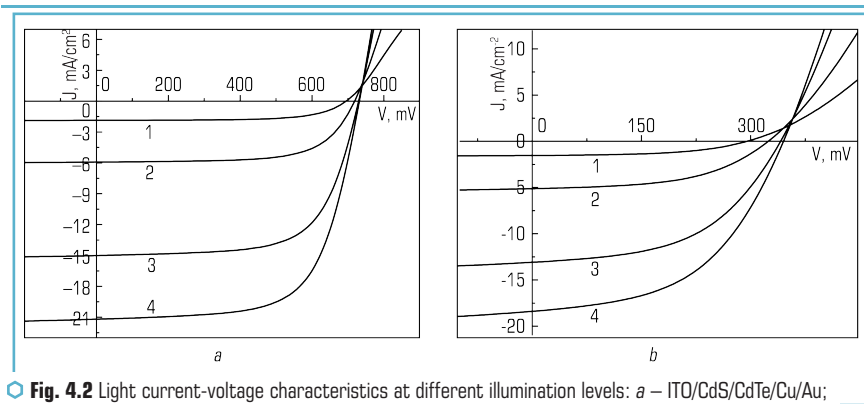


Fig. 4.2 Light current-voltage characteristics at different illumination levels: a – ITO/CdS/CdTe/Cu/Au; b – ITO/CdS/CdTe/Au; 1 – 10 mW/cm<sup>2</sup>; 2 – 30 mW/cm<sup>2</sup>; 3 – 70 mW/cm<sup>2</sup>; 4 – 100 mW/cm<sup>2</sup>

An analysis of the light diode characteristics shows that for a SC with a Cu/Au back contact, with increasing illumination, a traditional increase in the photocurrent density is observed (Table 4.1), which is due to an increase in the concentration of nonequilibrium charge carriers with an increase in the incident photon flux density. With an increase in illumination, the shunt resistance decreases, which is due to an increase in the specific conductivity of the base layer. The size of the series resistance does not depend enough on the illumination. This indicates that the predominant contribution to the value of the series resistance of the device structure is made by the resistance of the back and front contacts.

Table 4.1 Effect of illumination level on initial parameters and light diode characteristics of ITO/CdS/CdTe/Cu/Au

Parameters and characteristics	$P_e$ , mW/cm <sup>2</sup>									
	10	20	30	40	50	60	70	80	90	100
$J_{SC}$ , mA/cm <sup>2</sup>	1.9	3.8	5.94	8.3	10.3	12.8	15.0	17.0	19.5	21.2
$V_{nl}$ , mV	697	711	719	720	728	727	729	731	727	731
$FF$ , c.u.	0.66	0.67	0.67	0.67	0.67	0.663	0.66	0.66	0.66	0.66
Efficiency, %	8.7	9.1	9.49	10	10	10.29	10.37	10.23	10.36	10.19
$J_p$ , mA/cm <sup>2</sup>	1.87	3.8	5.95	8.4	10.3	12.8	15.1	17.0	19.5	21.3
$R_s$ , Ohm·cm <sup>2</sup>	<1	<1	<1	<1	<1	1.3	1.3	1.4	1.6	1.6
$R_w$ , Ohm·cm <sup>2</sup>	8250	4420	2390	2400	1280	1010	894	741	694	623
$A$ , c.u.	2.9	2.9	2.8	2.8	2.7	2.6	2.6	2.5	2.5	2.5
$J_0$ , 10 <sup>-7</sup> A/cm <sup>2</sup>	1.3	2.2	2.7	2.7	2.6	2.2	2.6	2.1	1.8	1.9

The effect of annealing at a temperature of 200 °C for 30 minutes on the initial characteristics of a SC with a Cu/Au back contact was also studied.

● **Table 4.2** Effect of rear contact annealing on the initial parameters of the ITO/CdS/CdTe/Cu/Au

Output parameters	$V_{nl}$ , mV	$J_{sc}$ , mA/cm <sup>2</sup>	FF	Efficiency, %
Before annealing	322	20.2	0.41	1.6
After annealing in air	723	22.2	0.54	8.8

It has been established that the efficiency is limited to 2 % after annealing in device structures. The decisive contribution to the limitation of efficiency is made by low values of the no-load voltage. The results obtained indicate that only annealing in a SC with a Cu/Au back contact leads to the formation of an effective tunnel contact. According to the literature data [28], this is due to the interfacial interaction of the copper film and the surface layer of tellurium, which leads to the formation of a degenerate  $Cu_{2-x}Te$  semiconductor. Without a degenerate semiconductor layer, in device structures with a Cu/Au back contact, as well as for a SC with an Au back contact, the through diode mode is implemented, which limits the value of the open-circuit voltage.

## 4.2 STUDY OF TANDEM AND BILATERALLY SENSITIVE SOLAR CELLS BASED ON CDS/CDTE

### 4.2.1 RESULTS OF INVESTIGATION OF TRANSPARENT REAR CONTACTS CU/ITO FOR DOUBLE-SIDED SENSITIVE $SnO_2:F/CDS/CDTE/CU/ITO$ SOLAR CELLS

A promising direction for increasing the efficiency of photoelectric conversion of solar energy and the ability to work stably for a long period of time is the development of tandem and bilaterally sensitive photoelectric converters (PECs). The development of multilayer tandem structures involves the use of several base layers with different band gaps. This makes it possible to efficiently convert solar radiation in a wide spectral range. Thus, high-energy photons are absorbed in the first base layer, the rest of the radiation enters the PEC located below with a base layer having a smaller band gap. The main requirements for the creation of tandem structures are the small thickness and transparent rear contact of the PEC with the wide-gap base layer [29]. This is necessary for the passage of the long-wavelength part of the spectrum through the base layer with minimal losses. For bilaterally sensitive photovoltaic converters, the main requirement is efficient conversion of solar radiation when illuminated from both sides. Given the high radiation resistance of cadmium telluride, it is promising to use bilaterally sensitive solar cells based on it for power supply of spacecraft. Since the back of the solar battery of the spacecraft is illuminated by solar radiation reflected from the body. Therefore, it is necessary to conduct research on the conditions for creating transparent rear electrodes for pho-

toelectric converters based on CdTe, intended for use in both tandem and bilaterally sensitive device structures.

The use of PV film PEC with CdTe and CuInSe<sub>2</sub> [30] base layers is promising for creating tandem structures. It is known that the band gap of CdTe is 1.46 eV [6], and the band gap of CuInSe<sub>2</sub> is 1.10 eV [31]. The combination of the energy structure of such PECs is able to provide efficient conversion of solar radiation, both in terrestrial and atmospheric conditions. However, the use of PEC based on CdTe in tandem structures is constrained by the difficulty of creating back contacts suitable for industrial production. This is due to the fact that only platinum has the electron work function necessary for the formation of an ohmic transition. Other metals with cadmium telluride form a Schottky barrier, which affects the efficiency of photovoltaic processes in solar cells based on it [32]. Therefore, the main approach to the creation of low-resistance electrodes is the formation of tunnel electrodes containing copper. However, the diffusion of copper into the base layer leads to degradation of the initial parameters of film solar cells based on CdS/CdTe. The authors of [33] proposed the creation of a rear contact without the use of copper. However, the efficiency of the studied samples did not exceed 6.2 %, and their degradation resistance was studied only for one year, which is not enough for operation in terrestrial and atmospheric conditions. The work [34] presents studies devoted to the creation of ohmic back contacts using an organic layer of the leading PEDOT-PSS polymer, which also does not contain copper. However, the efficiency of the obtained samples did not exceed 2 %. As shown by the authors, the low efficiency of experimental samples is due to the operation of the device structure in the mode of a through diode. The authors of [35] studied several types of metal oxides as a buffer layer for creating a high-quality rear contact for solar cells based on CdTe. But this approach complicates the adaptation to mass industrial production.

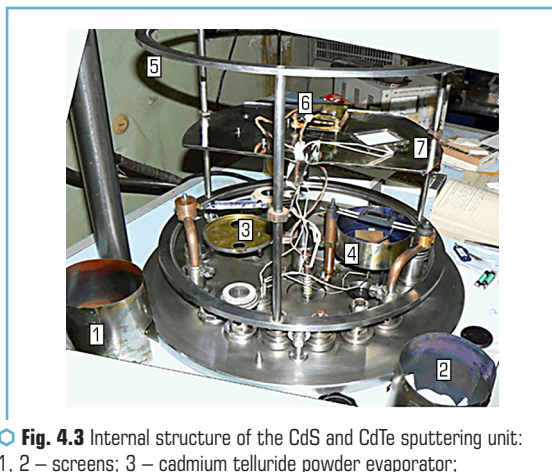
Thus, at present, the problem of creating efficient and transparent rear contacts with solar cells based on CdTe without the use of copper remains unresolved. Therefore, it is necessary to carry out research aimed at optimizing the design and technological solution for creating transparent rear electrodes.

#### 4.2.2 MATERIALS AND EQUIPMENT USED TO OBTAIN $\text{SnO}_2\text{:F/CDS/CDTE/CU/ITO}$ PHOTOVOLTAIC CONVERTERS

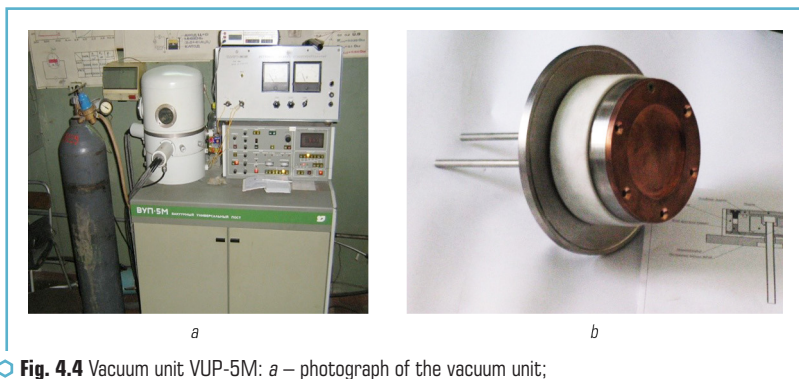
The studied device structures with a photoreceiving surface area of up to 2 cm<sup>2</sup> were obtained by thermal vacuum evaporation using a UVN67 vacuum unit with modified internal equipment [36–38]. The thickness of the CdTe base layer was 2.5 μm. The view of the internal equipment of the installation is shown in **Fig. 4.3**.

ITO films (indium and tin oxides) were deposited by nonreactive DC magnetron sputtering in a VUP-5M vacuum unit (**Fig. 4.4**). It should be noted that magnetron sputtering is one of the most promising methods for obtaining all transparent electrodes [15, 16]. This is due to the high degree

of accuracy in transferring the target composition to the substrate and the reproducibility and controllability of the magnetron sputtering process [39, 40].



○ **Fig. 4.3** Internal structure of the CdS and CdTe sputtering unit: 1, 2 – screens; 3 – cadmium telluride powder evaporator; 4 – cadmium sulfide powder evaporator; 5 – carousel; 6 – substrate heater; 7 – substrate holder



○ **Fig. 4.4** Vacuum unit VUP-5M: *a* – photograph of the vacuum unit; *b* – photograph of the material-saving magnetron

Since it is not possible to obtain efficient device structures without a copper interlayer, a nano-sized copper layer 2 nm thick was deposited on the surface of cadmium telluride before ITO was deposited. The minimization of the copper layer thickness was aimed at increasing the degradation resistance of the device structure.

According to [27], the technology of forming tunneling electrodes provides for chemical digestion before applying the electrode, during which a Te layer is formed, and the final stage is annealing, leading to the formation of the  $\text{Cu}_{2-x}\text{Te}$  phase, which is an innate conductor.

#### 4.2.3 MEASUREMENT TECHNIQUE AND ANALYTICAL PROCESSING OF LIGHT CURRENT-VOLTAGE CHARACTERISTICS

The measurement of light current-voltage characteristics (hereinafter – CVC) was carried out according to the method described in [41]. Imitation of solar radiation, close to the standard mode AM1.5, was carried out using a system of LEDs.

To measure the compensation method in the stationary mode of irradiation, close to the standard AM1.5, of the light current-voltage characteristics of SC samples.

Determination of the output parameters and light diode characteristics of photoelectric converters based on cadmium telluride was carried out according to the experimental light current-voltage characteristics. Analytical processing of the light CVCs of the studied PECs was carried out using a PC.

The relationship between the PEC efficiency and the light diode characteristics is implicitly described theoretically by the light CVC of the PEC:

$$J_l = J_p + J_0 \left\{ \exp \left[ \frac{e(V_l - J_l R_s)}{kT} \right] - 1 \right\} + (V_l - J_l R_s) / R_w, \quad (4.15)$$

where  $J_l$  – the current density flowing through the load;  $e$  – the electron charge;  $k$  – the Boltzmann constant;  $T$  – the temperature of the solar cell;  $V_l$  – voltage drop across the load.

According to the program, the analytical expression (4.15) for the light CVC turns into expressions having the form:

$$I_l = A_0 - A_1 V_l - A_2 \exp(A_3 V_l + A_4 I_l), \quad (4.16)$$

$$A_0 = (I_p + I_0) R_w / (R_s + R_w), \quad (4.17)$$

$$A_1 = 1 / (R_s + R_w), \quad (4.18)$$

$$A_2 = I_0 R_w / (R_s + R_w), \quad (4.19)$$

$$A_3 = e / (kT), \quad (4.20)$$

$$A_4 = e R_s / (kT). \quad (4.21)$$

Using expression (4.16) and the experimentally obtained values of  $I_l$  and  $V_l$ , by varying the values of the above coefficients  $A_0, A_1, A_2, A_3, A_4$  the best approximation of the experimental data  $I_l = I_l(V_l)$  of the curve described by the transformed theoretical expression (4.16) is achieved. Usually, during analytical processing, the standard deviation does not exceed  $10^{-8}$ , which corresponds to a relative error in determining the initial parameters and light diode characteristics at a level of no more than 1 %. After finding the indicated coefficients, which provide the best approximation, the initial parameters of the PEC are determined:  $I_{sc}$ ,  $V_{nl}$ ,  $FF$ ,  $R_w$ , efficiency. The light diode characteristics  $R_s$ ,  $R_w$ ,  $A$  and  $I_0$  are calculated from the found coefficients  $A_0, A_1, A_2, A_3, A_4$ , using relations (4.17)–(4.21) [42–44]. The error in determining the initial parameters and light diode characteristics is determined not only by the value of the standard deviation, but also by the error in the light CVC measurement.

#### 4.2.4 RESULTS OF THE STUDY OF LIGHT CURRENT-VOLTAGE CHARACTERISTICS OF $\text{SnO}_2\text{:F/CDS/CDTE/CU/ITO}$ PHOTOELECTRIC CONVERTERS

By analytical processing of the light CVCs (**Fig. 4.5**), the initial and light diode properties of the made solar cells were analyzed.

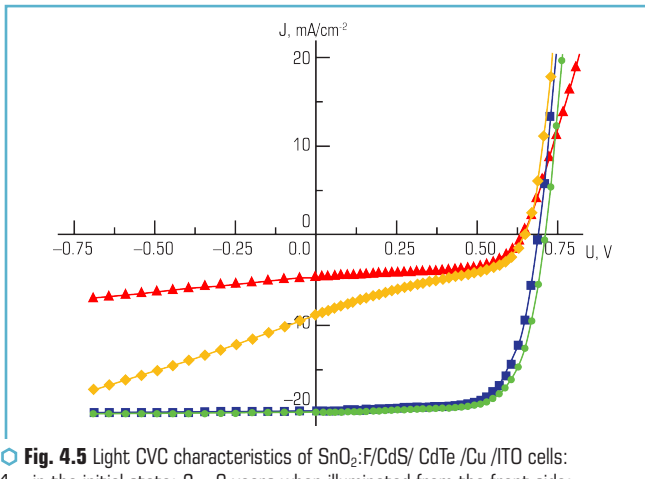


**Fig. 4.5** Light CVC characteristics of  $\text{SnO}_2\text{:F/CdS/CdTe/Cu/ITO}$  cells:  
1 – in the initial state; 2 – 8 years when illuminated from the front side;  
3 – in the initial state; 4 – ~ 8 years when illuminated from the back side

After taking the initial light CVCs under illumination from the front and back sides, the standards were kept at a constant light flux in a special chamber in the idle mode. Lighting was provided

by a 500 W incandescent lamp, the sample temperature was 80 °C. It was shown in [42] that such illumination regimes increase the degradation rate by a factor of 100. At certain intervals, conditionally corresponding to: 0; 0.5; 1.4; 3.6; 4.2; 5.4; 6.02 and 8 years, repeated measurements of light CVCs were made. **Table 4.1** presents the results of analytical processing of light CVC characteristics under illumination from the front side are shown in **Table 4.3**.

● **Table 4.3** Output parameters and light diode characteristics of ITO/CdS/CdTe/Cu/ITO PV cells when illuminated from the front side

$t, h$	0	0.5	1.4	3.6	4.2	5.4
$J_{sc}, \text{mA/cm}^2$	19.4	19.4	19.4	19.4	19.5	19.4
$V_{nl}, \text{mV}$	740	720	710	710	710	710
$FF, \text{c.u.}$	0.68	0.73	0.75	0.74	0.73	0.73
Efficiency, %	9.8	10.2	10.3	10.1	10.2	10.1
$J_p, \text{mA/cm}^2$	19.5	19.0	19.5	19.4	19.5	19.4
$R_s, \text{Ohm}\cdot\text{cm}^2$	1.6	1.2	0.5	0.3	0.7	0.4
$R_w, \text{Ohm}\cdot\text{cm}^2$	1031	911	882	965	821	922
$A, \text{c.u.}$	2.28	1.68	1.65	1.77	1.76	1.91
$J_0, 10^{-7} \text{A/cm}^2$	$6.2 \times 10^{-8}$	$1 \times 10^{-9}$	$9.7 \times 10^{-10}$	$3.3 \times 10^{-9}$	$2.5 \times 10^{-9}$	$9 \times 10^{-9}$

**Table 4.3** shows that at the beginning of the PEC operation and up to 1.4 years, there is an increase in efficiency from 9.9 % to 10.3 %, which is due to an increase in the filling factor of the light CVC from  $FF=0.68$  to  $FF=0.75$  against the background of an insignificant lowering the open circuit voltage from  $V_{nl}=740 \text{ V}$  to  $V_{nl}=710 \text{ V}$  and the short circuit current density from  $J_{sc}=19.5 \text{ mA/cm}^2$  to  $J_{sc}=19.4 \text{ mA/cm}^2$ . With a further increase in the operating time to 6 years, the efficiency slowly decreases to 10 %. Then the decrease in efficiency occurs faster and with an increase in operating time up to 8 years, a decrease in efficiency to 9.7 % is observed. The reduction in efficiency occurs as a result of a decrease in the filling factor of the light CVC from  $FF=0.75$  to  $FF=0.71$ , and the open-circuit voltage also continues to decrease slightly to 700 mV. The short circuit current density practically does not change. It should be noted that after 8 years of operation, the efficiency of the  $\text{SnO}_2:\text{F}/\text{CdS}/\text{CdTe}/\text{Cu}/\text{ITO}$  PEC practically coincides with the initial value, which indicates a high degradation resistance of the resulting heterosystems [45, 46].

An analysis of the worldwide diode characteristics of  $\text{SnO}_2:\text{F}/\text{CdS}/\text{CdTe}/\text{Cu}/\text{ITO}$  solar cells shows that initially, with an increase in operating time up to 1 year, the saturation diode current density decreases from  $J_0=1.6 \times 10^{-8} \text{ A/cm}^2$  to  $J_0=9.7 \times 10^{-10} \text{ A/cm}^2$ . At the same time, the diode ideality coefficient also decreases. With a further increase in the operating time to 7.5 years, the diode saturation current density increases by almost two orders of magnitude up to  $J_0=2.4 \times 10^{-8} \text{ A/cm}^2$ ,

the ideality factor also increases. This may be due to the fact that copper atoms, diffusing into the base layer at the grain boundary, reach the p-n transition region and partially shunt it. At the same time, the series resistance during almost the entire period of operation decreases from  $R_s=2.2 \text{ Ohm}\cdot\text{cm}^2$  to  $R_s=0.3 \text{ Ohm}\cdot\text{cm}^2$ , and only after 7 years of operation is its reverse increase to  $R_s=0.6 \text{ Ohm}\cdot\text{cm}^2$ . The shunt resistance first increases from  $R_w=850 \text{ Ohm}\cdot\text{cm}^2$  to  $R_w=960 \text{ Ohm}\cdot\text{cm}^2$ , and after four years it decreases to  $R_w=880 \text{ Ohm}\cdot\text{cm}^2$  with a subsequent return to the level  $R_w=960 \text{ Ohm}\cdot\text{cm}^2$ .

The light diode characteristics of  $\text{SnO}_2\text{:F/CdS/CdTe/Cu/ITO}$  solar cells improve at the beginning of operation, and after 7–8 years they deteriorate and return almost to their initial values. This behavior of the diode characteristics is responsible for the observed high degradation resistance.

Thus, the use of a copper layer 2 nm thick makes it possible to create a rear Cu/ITO tunnel contact without lowering the degradation resistance of the device structure. Since thin-film PECs are traditionally guaranteed stable efficiency for 5 years, it becomes obvious that the use of the proposed transparent rear electrodes in the conditions of industrial production of film PECs based on cadmium telluride becomes obvious [47].

The results of analytical processing of the experimental CVC under illumination from the back are presented in **Table 4.4**.

● **Table 4.4** Output parameters and light diode characteristics of ITO/CdS/CdTe/Cu/ITO PV cells under illumination from the back side

<b>t, h</b>	<b>0</b>	<b>1.4</b>	<b>3.6</b>	<b>5.4</b>	<b>6.0</b>	<b>8</b>
$J_{sc}, \text{mA}/\text{cm}^2$	4.7	7.5	6.7	6.7	6.9	7.0
$V_{nl}, \text{mV}$	650	660	660	650	650	630
$FF, \text{c.u.}$	0.55	0.42	0.39	0.39	0.36	0.32
Efficiency, %	1.7	2.1	1.8	1.7	1.6	1.4
$J_p, \text{mA}/\text{cm}^2$	4.7	7.7	6.9	6.8	7.1	7.2
$R_s, \text{Ohm}\cdot\text{cm}^2$	3.2	4.3	4.6	1.5	3.8	3.1
$R_w, \text{Ohm}\cdot\text{cm}^2$	438	146	155	150	132	112
$A, \text{c.u.}$	1.9	1.2	1.3	1.3	1.1	1.1
$J_0, 10^{-7}\text{A}/\text{cm}^2$	$6.9\times 10^{-9}$	$3.1\times 10^{-13}$	$3.8\times 10^{-12}$	$1.2\times 10^{-11}$	$3.6\times 10^{-13}$	$3.6\times 10^{-13}$

As can be seen from **Table 4.4**, the PEC efficiency when illuminated from the back side is significantly less than when illuminated from the front side. The ratio between the efficiency during the entire period of operation remains in the range from 5 to 7, reaching a minimum difference when the efficiency when illuminated from the front and rear sides reaches maximum values. Moreover,

the relative increase in efficiency at the beginning of operation with illumination from the back side is greater (23 % compared with the initial value) than with illumination from the front side (4 % compared with the initial value). The lower values of efficiency are primarily due to the lower values of the filling factor of the light CVC and the lower short-circuit current density. When illuminated from the back side in the initial state, the filling factor of the light CVC is  $FF=0.56$ , and after 7.5 years it decreases to  $FF=0.32$ . It should be noted that when illuminated from the front side, the fill factor decreases slightly. The short-circuit current density in the initial state when illuminated from the back side is 4 times less than when illuminated from the front side. After a year of operation, the ratio of these currents becomes approximately equal to 2.6 and remains unchanged further. The open-circuit voltage, both when illuminated from the front side and when illuminated from the back side, changes slightly and differs from the value for front illumination by (0.05–0.1) V.

Thus, the study of the light current–voltage characteristics of the  $\text{SnO}_2:\text{F}/\text{CdS}/\text{CdTe}/\text{Cu}/\text{ITO}$  PEC showed that a decrease in the thickness of the copper layer deposited on the CdTe surface to  $\sim 2$  nm made it possible to create degradation-resistant solar cells with a transparent rear contact.

The fixed evolution of the output parameters with a change in the direction of illumination is due to a change in the light diode characteristics. The decrease in the short circuit current density is due to the corresponding decrease in the photocurrent density. The fixed decrease in  $J_p$  when the direction of illumination changes is due to the fact that when illuminated from the front side, active generation of nonequilibrium charge carriers occurs near the p-n junction or inside its depletion region. As a result, most of it is generated under the action of light from nonequilibrium charge carriers and falls into the region of the built-in electric field of the p-n junction, where, after separation, a photocurrent is formed. When the device structure is illuminated from the rear, the nonequilibrium carrier generation region is separated from the p-n transition region. Therefore, a significant part of the generated nonequilibrium charge carriers as a result of volume and surface recombination do not contribute to the creation of a photocurrent.

When illuminated from the back, the series resistance is several times higher than when illuminated from the front, and does not decrease with increasing operating time. The density of the diode saturation current when illuminated from the rear side decreases by almost three orders of magnitude and practically does not change with an increase in the operating time. When changing the direction of illumination from the front to the back, the shunt resistance decreases several times. In addition, with an increase in the operating time, a decrease in the shunt resistance is observed. So, in the initial state, the ratio of the shunt resistance in front lighting to the shunting resistance in back lighting was 2 times, and by the end of operation it quickly increased to 8 times.

When analyzing the world-class diode characteristics, it is necessary to take into account the possibility of realizing the inverted diode regime presented in [48] in the structure under study, when the rear contact is a diode connected in series with respect to the main diode. The energy structure of the diodes is affected by the direction of illumination, which causes a change in the series and shunt resistance, as well as a change in the diode saturation current density. If the main contribution to the value of  $J_0$  is made by the energy structure of the main separating barrier,

the decrease in  $J_0$  when the direction of illumination changes from front to rear is due to an exponential decrease in the intensity of its illumination.

This, in turn, reduces the concentration of nonequilibrium charge carriers near the p-n junction. If the main contribution to the shunt resistance is made by the barrier properties of the back contact, it becomes obvious that this diode characteristic decreases when the direction of illumination changes from front to back. When the rear barrier is illuminated in the space charge region, the concentration of nonequilibrium charge carriers increases, which leads to a decrease in the shunt resistance as a result of a decrease in the thickness of the depletion layer. The series resistance is higher when illuminated from the rear, since in this case a significant amount of nonequilibrium charge carriers is not generated near the main p-n junction, and the depletion region increases, which leads to an increase in series resistance.

The evolution of the global diode characteristics with an increase in the operating time is due to the diffusion of copper from the nanosized interlayer into the volume of the base layer, which can occur according to the grain boundary and volume mechanisms.

Since copper is an acceptor impurity for cadmium telluride, its diffusion in the volume of the base layer of cadmium telluride leads to a decrease in the resistivity of the base layer and, accordingly, to a decrease in the PEC series resistance [49]. Diffusion of the acceptor into the grain boundary surface leads to the formation of a p-p + transition between the boundary and the bulk of the grain. Such potential barriers push nonequilibrium electrons into the bulk of the grain, generated under the action of light, by their built-in electric field, which reduces the negative effect of the grain boundary surface as a region with a high concentration of recombination centers. This approach makes it possible to expand the range of materials for creating rear contact with CdTe-based solar cells.

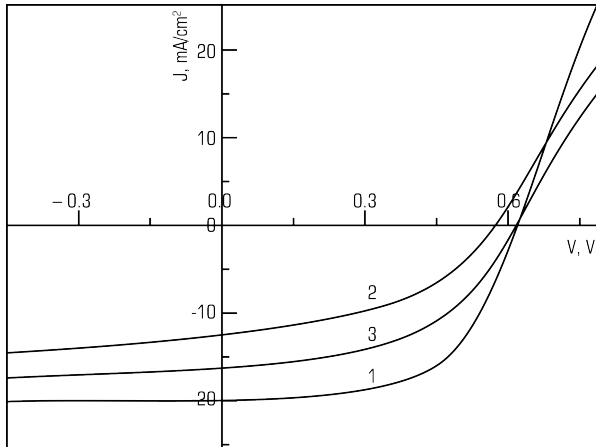
The obtained low efficiency values of the  $\text{SnO}_2\text{:F/CdS/CdTe/Cu/ITO}$  PEC under illumination from the side of the transparent rear contact require a more detailed analysis and further studies aimed at optimizing the thickness of the base layer.

#### 4.2.5 THE RESULTS OF THE STUDY OF THE INITIAL PARAMETERS OF THE ITO/CDS/CDTE/CU/ITO SC UNDER BILATERAL IRRADIATION

To quantify the effect of bilateral irradiation on the efficiency of electric power generation, comparative studies of the CdS/CdTe/Cu/ITO light CVC were carried out under irradiation from the back and front sides and simultaneous irradiation (**Fig. 4.6**).

By analytical processing of the light CVCs of the studied samples, the initial parameters were obtained for various types of irradiation, which are given in **Table 4.5**.

As can be seen from **Table 4.5**, when irradiated from the rear side, a significant decrease in the values of  $J_{sc}$  and  $V_{nl}$  is observed and, accordingly, is accompanied by a significant decrease in efficiency. However, simultaneous irradiation on both sides shows high results of the initial parameters.



● Fig. 4.6 Light CVC of CdS/CdTe/Cu/ITO SCs: 1 – when irradiation from the rear side; 2 – when irradiated from the front side; 3 – when simultaneous irradiation from the back and front sides

● Table 4.5 Initial parameters of the ITO/CdS/CdTe/Cu/ITO SCs under various irradiation options

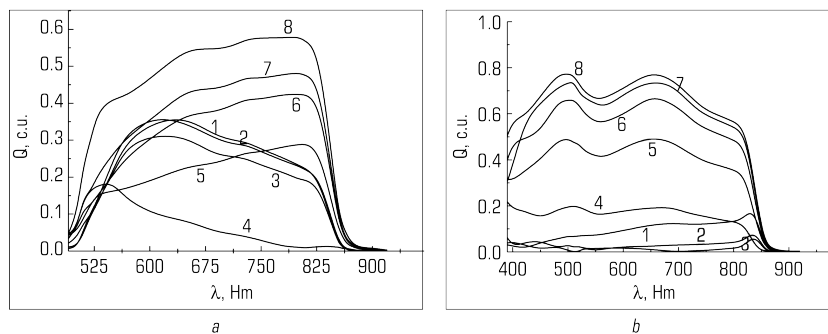
#### Irradiation direction

SC initial parameters	from the front side	from the back side	on both sides at the same time	
$J_{sc}$ , (mA/cm <sup>2</sup> )	19.6	12.5	32.4	32.1*
$V_{nl}$ , (mV)	620	570	610	–
FF, c.u.	0.59	0.44	0.50	–
Efficiency, %	7.17	3.13	9.88	–

Note: \* are the initial parameters of the theoretical light CVC obtained by adding two experimental light CVC under illumination from the back

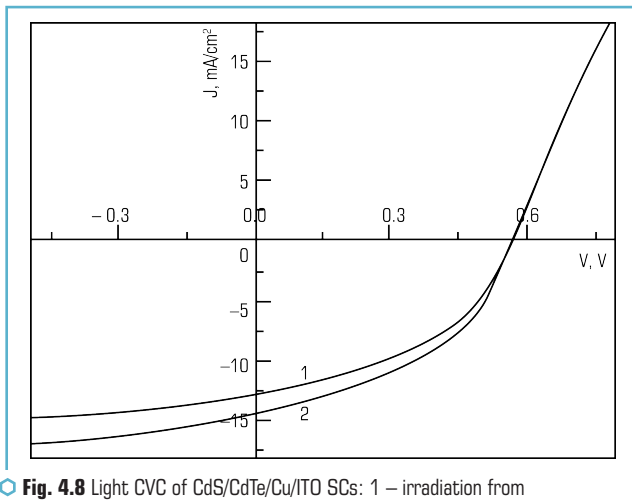
#### 4.2.6 RESULTS OF STUDYING THE SPECTRAL DEPENDENCES OF THE ASSEMBLY FACTOR OF ITO/CDS/CDTE/CU/ITO SCS AT VARIOUS BIAS VOLTAGES

To analyze the possibility of using the developed SC based on ITO/CdS/CdTe/Cu/ITO in tandem device structures, let's study the spectral dependences of the removal factor at various bias voltages and various irradiation directions. On the basis of the obtained spectral dependences, the effect of the space-charge region of the rear contact on the efficiency of photoelectric processes in the base layer of a SC based on ITO/CdS/CdTe/Cu/ITO was analyzed (Fig. 4.7).



○ **Fig. 4.7** Spectral dependences of the assembly factor of CdS/CdTe/Cu/ITO SCs with a base layer thickness of  $1 \mu\text{m}$  at various bias voltages (1 – 0 V, 2 – 0.5 V, 3 – 0.6 V, 4 – 0.7 V, 5 – 0.8 V, 6 – 0.9 V, 7 – 1.1 V, 8 – 1.2 V): a – when irradiated from the front side; b – when irradiated from the back side

To quantify the contribution of incomplete absorption to a decrease in the photocurrent density, let's study the CdS/CdTe/Cu/ITO light CVCs with a base layer thickness of  $1 \mu\text{m}$  under illumination from the rear side (**Fig. 4.8**).



○ **Fig. 4.8** Light CVC of CdS/CdTe/Cu/ITO SCs: 1 – irradiation from the rear side; 2 – rear-front irradiation

The initial parameters of the SC during the analytical processing of light CVC are presented in **Table 4.6**.

● **Table 4.6** Initial parameters of the CdS/CdTe/Cu/ITO SCs with a base layer thickness of 1  $\mu\text{m}$  for various irradiation options

SC initial parameters	Irradiation direction		
	Rear side	rear-front	front
$J_{sc}$ , (mA/cm <sup>2</sup> )	12.5	14.1	19.7
$V_{oc}$ , (mV)	570	571	666
FF, c.u.	0.44	0.43	0.60
Efficiency, %	3.1	3.4	7.8

When conducting such studies, a mirror was installed on the front side under illumination from the back side, which allowed the radiation transmitted through the SC to be directed again to the base layer from the front side. Thus, the loss of electric power generated by the SC due to incomplete absorption of light when illuminated from the back was analyzed experimentally.

#### 4.2.7 THE RESULTS OF THE STUDY OF THE INITIAL PARAMETERS OF THE ITO/CDS/CDTE/CU/ITO SCS AS PART OF TANDEM SCS

The developed ITO/CdS/CdTe/Cu/ITO SCs were tested as part of tandem SCs with a narrow-gap layer based on copper and indium diselenide. Such solar cells were made at the Swiss Institute of Technology. Mo/CuInSe<sub>2</sub>/CdS/ZnO/ZnO:Al/Ni SCs were produced on glass substrates and had a front configuration. Illumination of such device structures is carried out from the side of Ni comb contact. The light CVCs of such device structures were studied when the ITO/CdS/CdTe/Cu/ITO SCs with a base layer thickness of 1  $\mu\text{m}$  and an efficiency of 7.8 % was located on the illuminated surface (**Fig. 4.9**).

The initial parameters of characteristic samples of Mo/CuInSe<sub>2</sub>/CdS/ZnO/ZnO:Al/Ni SCs and the ITO/CdS/CdTe/Cu/ITO – Mo/CuInSe<sub>2</sub>/CdS/ZnO/ZnO:Al/Ni tandem photovoltaic converter are presented in **Table 4.7**.

As can be seen from **Table 4.7**, placing an ITO/CdS/CdTe/Cu/ITO SC on a Mo/CuInSe<sub>2</sub>/CdS/ZnO/ZnO:Al/Ni surface leads to a significant decrease in the efficiency of the latter.

Thus, we have analyzed the parameters and efficiency of the device structure of the ITO/CdS/CdTe/Cu/ITO SC, which were obtained by analytical processing of light CVC. It has been established that the resulting light CVC of the SC when illuminated from both sides is the sum of the light CVC when illuminated from the rear and front sides.

However, double-sided lighting allows to increase the generated electrical power by 43 %. This reduces the area of the corresponding one-sided SC, which makes it possible to expand the possibilities of their use in the prevention of emergencies in the case of a limited deployment area.

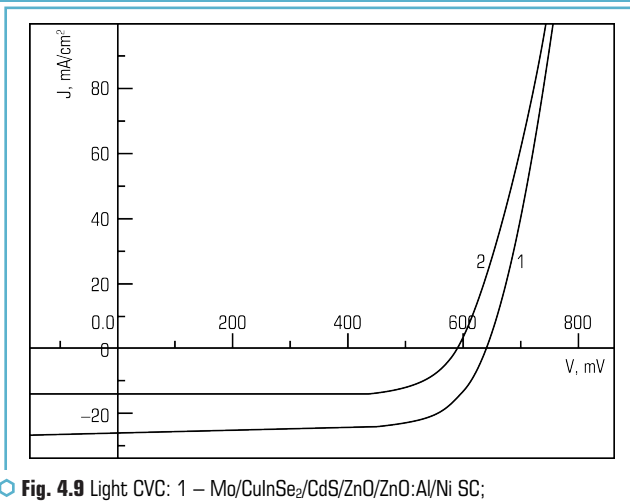


Fig. 4.9 Light CVC: 1 – Mo/CuInSe<sub>2</sub>/CdS/ZnO/ZnO:Al/Ni SC; 2 – when ITO/CdS/CdTe/Cu/ITO is located on its front surface

Table 4.7 Initial characteristics of the solar parts of the tandem structure

SC parameters	CuInSe <sub>2</sub>	CuInSe <sub>2</sub> / CdTe	CdTe
$J_{SC}$ , (mA/cm <sup>2</sup> )	25,9	13,8	19,7
$V_{nl}$ , (mV)	634	590	666
$FF$ , c.u.	0,68	0,74	0,60
Efficiency, %	11,2	6,0	7,8

An analysis of the spectral dependences of the ITO/CdS/CdTe/Cu/ITO SC collection coefficient at various bias voltages has been carried out. It was found that in the absence of a shear stress, the maximum in the spectral dependence is observed at a wavelength of 0.65  $\mu\text{m}$ , then a decrease in the photoresponse is observed, so that the area under the spectral dependence decreases by 20 %.

Since the area under the spectral dependence of the quantum efficiency coefficient is proportional to the short-circuit current density, the efficiency of the device structure also decreased by 20 rel. %. Such a significant decrease in the efficiency of photoelectric processes can probably be due either to the negative effect of surface recombination at the rear contact or to incomplete absorption in the base layer due to the small thickness of the base layer.

Analysis of the **Table 4.6** shows that if the radiation transmitted through the solar cell, when illuminated from the back side, is again directed to the front surface with the help of a mirror,

this leads to an increase in electric power by  $0.3 \text{ mW/cm}^2$ . The increase in efficiency is due to an increase in the short-circuit current density by  $1.6 \text{ mA/cm}^2$  at constant values of the open-circuit voltage and the filling factor of the light CVC. Relative to the value of the short-circuit current density during irradiation from the front side, the increase in this initial parameter is 8 %. Thus, it has been experimentally shown that, in reducing the efficiency of photoelectric processes, the contribution of incomplete light absorption in the base layer to its photosensitivity practically coincides with the negative contribution of the rear contact.

With an increase in the forward bias, the area of the space charge of the main separating barrier, where there is a built-in electric field that accelerates the movement of electrons, decreases. This leads to a decrease in the assembly efficiency of nonequilibrium charge carriers generated under the action of light due to a decrease in the region of the semiconductor where they drift in an electric field. A decrease in efficiency is experimentally observed in the analysis of spectral dependences. With increasing voltage, a decrease in  $Q(\lambda)$  is observed in the entire spectral range of the photosensitivity. In this case, the largest decrease is observed for nonequilibrium charge carriers generated under the action of photons from the long-wavelength part of the spectrum. With an increase in the wavelength, the depth of light absorption increases, which leads to the removal of the active generation region from the region of the separating barrier. There is also an increase in the negative effect on the volume recombination collection coefficient during the diffusion of charge carriers from the generation region to the separation region.

At a voltage of 0.7 V, which corresponds to the open circuit voltage, the photosensitivity becomes equal to zero, since the external electric field becomes equal to the internal field of the separating barrier. Since these electric fields have the opposite content, the process of separation of nonequilibrium carriers stops. With a further increase in the bias voltage, its drop is carried out on the rear diode, connected in the opposite direction. Therefore, the rear diode begins to separate nonequilibrium charge carriers. As a result, the shape of the spectral dependence of the photorecall changes. Nonequilibrium charge carriers, generated under the action of photons from the long-wavelength part of the spectrum, begin to make the greatest contribution to the creation of photoresponse, since the region of their generation is located near the fission region. When illuminated from the rear side (**Fig. 4.7, b**), the maximum in the spectral dependence is observed when photons are absorbed from the long-wavelength region of the spectrum, which indicates a high surface recombination at the rear contact. Indeed, nonequilibrium charge carriers, when illuminated from the back side, are generated near the back surface. If this surface is characterized by a high rate of surface recombination, then the contribution of charge carriers generated near the back to the photorecall is minimized, which is observed experimentally. With an increase in the bias voltage, the energy structure of the rear contact is optimized and the depletion region grows, which causes an increase in the photoresponse over the entire spectral range of the photosensitivity.

An analysis of the initial parameters of the ITO/CdS/CdTe/Cu/ITO – Mo/CuInSe<sub>2</sub>/CdS/ZnO/ZnO: Al/Ni tandem structure shows that the absorption of a part of the incident radiation in the

ITO/CdS/CdTe/Cu/ITO SC leads to a decrease in the efficiency SC Mo/CuInSe<sub>2</sub>/CdS/ZnO/ZnO:Al/Ni from 11.2 % to 6.0 %. This decrease in efficiency occurs due to a decrease in the short circuit current density from 25.9 mA/cm<sup>2</sup> to 13.8 mA/cm<sup>2</sup>.

In this case, the open-circuit voltage decreases slightly, and the filling factor of the light CVC increases. The results obtained are in good agreement with those shown in **Fig. 4.2** by the spectral dependence of the transmittance of the ITO/CdS/CdTe/Cu/ITO SC. Since the short circuit current density linearly depends on the intensity of the incident radiation, and the open circuit voltage depends on it logarithmically.

It should be noted that, despite a significant decrease in the efficiency of the Mo/CuInSe<sub>2</sub>/CdS/ZnO/ZnO:Al/Ni SC when it is darkened by the ITO/CdS/CdTe/Cu/ITO SC, the efficiency of the tandem structure is noticeably higher than that of such CEs separately and amounts to 13.8 %.

### 4.3 STUDY OF SOLAR CELLS BASED ON CDS/CDTE ON A FLEXIBLE SUBSTRATE AS PART OF A MODULE

#### 4.3.1 DEVELOPMENT OF A METHOD FOR OBTAINING A CDS/CDTE/CU/AU MODULE ON A FLEXIBLE SUBSTRATE DESIGNED FOR BACKUP POWER SUPPLY OF EMERGENCY PREVENTION SYSTEMS

Thin film solar cells can generally be designed in two structures, known as superstrate and substrate, depending on the direction of light entry into the bulk of the device structure. In film solar cells of the "superstrate" type, light enters the cell from the side of the substrate on which the base layers are deposited and then passes into the volume of the device structure. For film solar cells of the "substrate" type, the light comes from the side opposite to the substrate. Thus, for superstrate SCs, the substrate must be transparent in order to transmit enough light into the volume of the device structure. Therefore, for the most part, it is the "superstrate" type that is used to create efficient solar cells based on CdTe [50]. While metal substrates can only be used for the "substrate" structure, polymer substrates are used in both cases depending on their transparency [51]. At present, the highest efficiency of film solar cells based on CdTe on a flexible substrate in the implementation of the "substrate" type reaches 13.8 % [52]. For film elements of the "substrate" type, 7.3 % when using a polymer and 7.8 % when using a metal foil, while the predicted theoretical maximum for CdTe-based SC is almost 30 % [53].

It is believed that with the superstrate configuration it is possible to obtain more efficient solar cells. This is due to the "chloride" treatment, which results in a decrease in the electrical resistivity of CdTe due to the generation of ClTe–VCd acceptors. In [45, 54], the use of "chloride" treatment made it possible to obtain experimental samples of solar cells with an efficiency of more than 10 %, but solar cells were fabricated on glass substrates. In the case of "substrate", "chloride" treatment can only be applied to CdS layers [34, 55]. In such a case,

the crystallinity of CdTe is not optimized. To create flexible solar cells, several materials are used as substrates, each of which has advantages and disadvantages. Among metals, molybdenum, titanium and stainless steel are most widely used, and among polymers – polyamide, polyethylene terephthalate and polyethylene naphthalate. The author of [56] used molybdenum as a flexible substrate. However, the efficiency of the obtained samples did not exceed 5 %, which is due to the complexity of forming an ohmic contact of such device structures. In [57], molybdenum and stainless steel were used as flexible substrates. The resulting device structures were studied by X-ray diffractometry, which made it possible to establish that, in addition to the difficulty of forming a rear contact, a limiting factor is the presence of defects in the form of dislocations in the base layer. In [58], Upilex polyimide films were used as substrates, which can withstand high temperatures (450 °C). The obtained results of the study demonstrated low efficiency values, which, according to the authors, is associated with inefficient radiation absorption in the polyamide substrate.

Thus, in the case of creating film solar cells based on CdTe on flexible substrates, the efficiency of device structures is limited by two groups of factors: firstly, it is the difficulty in creating a high-quality back contact, and secondly, significant absorption of the visible part of the spectrum when passing through the substrate .

### 4.3.2 PREPARATION OF SAMPLES OF THE ITO/CDS/CDTE/CU/AU MODULE ON A POLYAMIDE SUBSTRATE

The tested solar module based on CdS/CdTe consisted of four micromodules connected in parallel. Each micromodule consisted of five solar cells connected in series (**Fig. 4.10**). A set of metal masks was used to manufacture the module (**Fig. 4.11**). This method is more economical than photolithography. The module was fabricated on polyamide substrates, Kapton brand, manufactured by DuPont, amber color, 50 µm thick, by magnetron sputtering of the target [59]. The target was a compressed mechanical mixture of In<sub>2</sub>O<sub>3</sub> (90 wt. %) and SnO<sub>2</sub> (10 wt. %).

ITO films were formed at a deposition temperature of 300 °C. For the deposition of ITO films, a mask was used without separation into separate electrodes. The initial partial pressure was 104 Pa. The specific power of the magnetron was 1.5 W/cm<sup>2</sup>, which corresponds to the range of values commonly used to obtain transparent and electrically conductive ITO films [60]. ITO sputtering was carried out in an argon-oxygen mixture at a pressure of  $8 \times 10^{-1}$  Pa. Under such conditions, layers were formed with a surface resistance of 10 Ohm/□ and an average transmittance in the visible spectral range of about 90 %, which is achieved by reducing their thickness to 0.1 µm [60].

The same mask was used to apply the cadmium sulfide and telluride layers. The deposition of these layers was carried out in a single technological cycle by thermal vacuum deposition from graphite evaporators at an initial vacuum of 104 Pa without its excitation.



Fig. 4.10 Appearance of the solar cell module



Fig. 4.11 The system of masks for the module manufacture

The resulting instrumental heterosystems were subjected to the "chloride" treatment standard for this type of SC. In this case, smaller mask sizes were used. This is due to the fact that

cadmium telluride layers were used as dielectric layers separating the elements from each other, which are not affected by cadmium by the chloride layer and, therefore, were not subjected to "chloride" treatment, which reduces series resistance. To implement the "chloride" treatment, CdCl<sub>2</sub> films were deposited on the surface of the CdTe layers by thermal evaporation without heating the substrate. It is well known that "chloride" treatment [34] causes an increase in efficiency by several times. As a result of such treatment, the electrical resistivity of CdTe decreases due to the generation of ClTe–VCd acceptors with a concentration of about 10<sup>14</sup> cm<sup>-3</sup>, which reduces  $R_s$ . In addition, during such treatment, recrystallization of the base layer is observed, in which the CdTe columnar structure with a small grain size is transformed into a free orientation structure with large grain sizes. As a result, the probability of partial shunting of the separating barrier by the grain-boundary surface decreases, which causes an increase in  $R_w$ . Then the obtained multilayer film systems ITO/CdS/CdTe/CdCl<sub>2</sub> were annealed in air in a closed volume at a temperature of 430 °C for 25 min. To remove the reaction products, the annealed samples were subjected to digestion in a 5 % bromine solution in methanol.

To form the rear electrodes of the SC, two-layer Cu/Au electrical contacts were deposited on the etched surface of cadmium telluride in a vacuum setup by thermal evaporation. Since it is impossible to obtain effective device structures without a copper interlayer, a nanosized copper layer 2 nm thick was deposited on the surface of cadmium telluride. The minimization of the copper layer thickness was aimed at increasing the degradation resistance of the device structure.

### 4.3.3 RESULTS OF THE STUDY OF THE LIGHT CURRENT-VOLTAGE CHARACTERISTICS OF CDS/CDTE/CU/AU MICROMODULES ON A FLEXIBLE POLYAMIDE SUBSTRATE

The initial parameters of the micromodules included in the ITO/CdS/CdTe/Cu/Au module with serial connection of elements were obtained by analytical processing of the light CVCs (**Table 4.8**).

● **Table 4.8** Initial parameters of ITO/CdS/CdTe/Cu/Au micromodules with serial connection of solar cells

Micromodule	$V_{oc}$ , mV	$J_{sc}$ , mA/cm <sup>2</sup>	FF	Efficiency, %
M5_1	2449	2.8	0.59	4.0
M5_2	3489	2.7	0.39	3.7
M5_3	3572	2.8	0.54	5.3
M5_4	3052	2.1	0.56	3.5

The light CVC of the micromodules, measured at a light flux power of 100 mW/cm<sup>2</sup> and with a series connection of solar cells, are shown in **Fig. 4.12, 4.13**.

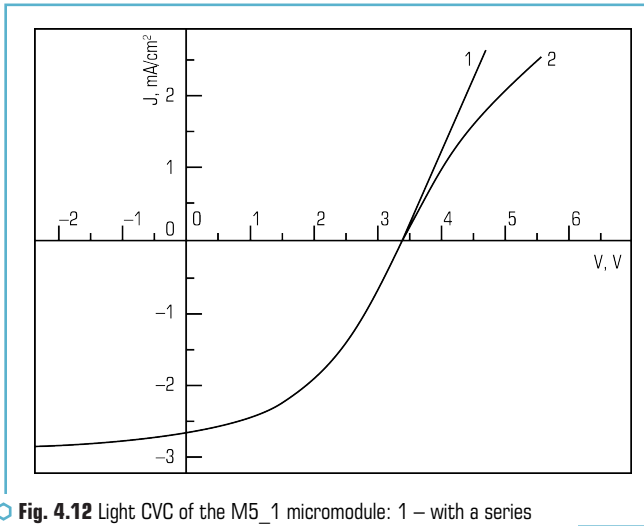


Fig. 4.12 Light CVC of the M5\_1 micromodule: 1 – with a series connection of four SCs; 2 – with five solar cells are connected in series

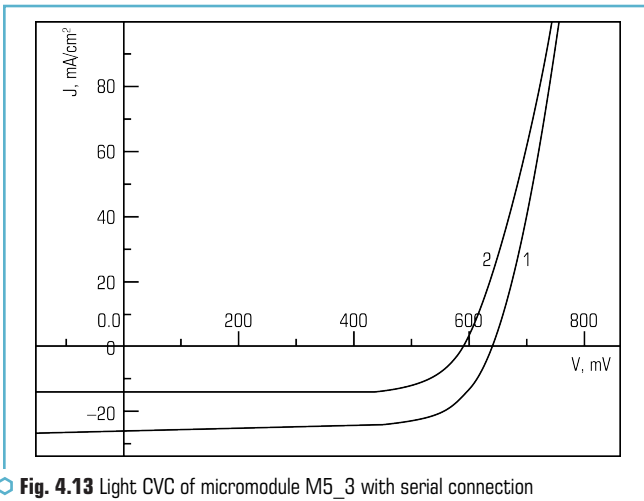


Fig. 4.13 Light CVC of micromodule M5\_3 with serial connection of five solar cells

As can be seen from **Table 4.8**, when the elements in the micromodule are connected in series, the efficiency of the micromodules reaches the maximum efficiency at the level of 5.3 %.

#### 4.3.4 THE RESULTS OF THE STUDY OF THE EFFECT ON THE EFFICIENCY OF MICROMODULES ON A FLEXIBLE POLYAMIDE SUBSTRATE OF THE INITIAL PARAMETERS OF THE CONSTITUENT ELEMENTS AND CONDITIONS FOR OBTAINING EXPERIMENTAL SAMPLES

By analytical processing of light CVCs, the initial parameters and light diode characteristics of the studied solar cells were obtained separately and when they were connected in series as part of a micromodule.

The results obtained are presented in **Tables 4.9, 4.10**, where C is a single SC, C2-C5 is a micromodule M5\_1 when four SCs are connected in series, C1-C5 is a micromodule when five SCs are connected in series.

As can be seen from **Tables 4.9** and **4.10**, the solar cell in the micromodule M5\_1 has the highest efficiency at the level of 8.4 %. However, the maximum efficiency of the entire micromodule is limited to 4.9 %.

● **Table 4.9** Output parameters and LED characteristics of micromodule SC M5\_1

Sample	C1	C2	C3	C4	C5	C2-C5	C1-C5
$V_{nl}$ , mV	97	748	755.5	133	752	2389	2486
$J_{SC}$ , mA/cm <sup>2</sup>	10.6	16.6	18.2	12.6	16.2	3.4	2.7
$FF$ , c.u.	0.27	0.61	0.61	0.26	0.59	0.59	0.58
Efficiency, %	0.3	7.5	8.4	0.4	7.1	4.9	3.9
$R_s$ , Ohm·cm <sup>2</sup>	4.1	8.77	8.47	3.03	8.77	186	239
$R_{ws}$ , Ohm·cm <sup>2</sup>	9.4	498	673	808	623	7×103	1×105
$J_0$ , A/cm <sup>2</sup>	9×10 <sup>-4</sup>	5×10 <sup>-11</sup>	4×10 <sup>-11</sup>	9×10 <sup>-6</sup>	6×10 <sup>-9</sup>	2×10 <sup>-14</sup>	2×10 <sup>-14</sup>
$A$ , c.u.	1.8	1.5	1.5	1.1	2.0	3.7	3.8
$J_p$ , mA/cm <sup>2</sup>	18.4	16.7	18.4	17.3	16.5	3.5	2.8

The study of the initial parameters of micromodules in the composition of the module on a polyamide substrate showed that the maximum efficiency (**Table 4.8**) is observed for the M5\_3 micromodule at the level of 5.3 %. Serial connection of solar cells in micromodules M5\_1 made it possible to obtain an efficiency of 3.9 %. Such a low efficiency value for the micromodule M5\_1 compared to the micromodule is due to M5\_3 with a low value of  $V_{nl}$ . The presumably low  $V_{nl}$  value for the M5\_1 micromodule is due to the shunting of the solar cells in the micromodule. This

assumption was confirmed by analyzing the initial parameters and light diode characteristics of individual solar cells of modules M5\_1 and M5\_3. An analysis of the initial parameters and light diode characteristics of individual solar cells of modules M5\_1 and M5\_3 showed that the first of the micromodules (M5\_1) had two practically shunted solar cells. The second micro-module (M5\_3) had one solar cell with a significantly lower efficiency.

● **Table 4.10** Output parameters and LED characteristics of micromodule SC M5\_3

Sample	C1	C2	C3	C4	C5	C1-C5
$V_{nl}$ , mV	752	762	552	758	741	3582
$J_{sc}$ , mA/cm <sup>2</sup>	15.2	16.7	16.9	17.8	16.9	2.7
$FF$ , c.u.	0.54	0.61	0.28	0.60	0.55	0.55
Efficiency, %	6.2	7.7	2.6	8.1	6.8	5.3
$R_s$ , Ohm·cm <sup>2</sup>	5.6	5.7	12.8	6.3	10.1	243
$R_w$ , Ohm·cm <sup>2</sup>	238	476	24	520	400	15630
$J_0$ , A/cm <sup>2</sup>	$3 \times 10^{-7}$	$5 \times 10^{-8}$	$6 \times 10^{-8}$	$2 \times 10^{-8}$	$7 \times 10^{-9}$	$5 \times 10^{-8}$
$A$ , c.u.	2.8	2.3	2.0	2.2	2.0	2.8
$J_p$ , mA/cm <sup>2</sup>	15.6	16.9	25.9	18.0	17.3	2.8

Analysis of the **Table 4.9** shows that for individual solar cells of the first micromodule, the light diode characteristics and initial parameters changed in the following intervals:  $R_s = (3-9)$  Ohm·cm<sup>2</sup>,  $R_w = (9-620)$  Ohm·cm<sup>2</sup>,  $J_0 = (4 \times 10^{-11}-9 \times 10^{-4})$  A/cm<sup>2</sup>,  $V_{nl} = (97-755)$  mV,  $J_{sc} = (10.6-18.2)$  mA/cm<sup>2</sup>,  $FF = (0.26-0.61)$ , efficiency = (0.3-8.4) %, for the second micromodule –  $R_s = (5.5-10)$  Ohm·cm<sup>2</sup>,  $R_w = (24-520)$  Ohm·cm<sup>2</sup>,  $J_0 = (7 \times 10^{-9}-3.0 \times 10^{-7})$  A/cm<sup>2</sup>,  $V_{nl} = (550-760)$  mV,  $J_{sc} = (15-17.8)$  mA/cm<sup>2</sup>,  $FF = (0.28-0.6)$ , efficiency = (2.6-8.1) %.

Thus, it can be argued that the low efficiency of micromodules in comparison with the efficiency of single solar cells in the micromodule is due to a decrease in all initial parameters. The creation of a Cu/Au tunnel back contact made it possible to obtain high  $V_{nl}$  values for individual solar cells, but as part of a micromodule it is limited to a shunted solar cell. The greatest role in reducing the efficiency of the entire micromodule is played by a significant decrease in  $J_{sc}$ , both for the first and second micromodules. This circumstance may be due to the inefficient absorption of radiation when passing through the dark yellow polyamide film. Therefore, for further research, it is necessary to focus on reducing the thickness of the polyamide film.

## CONCLUSIONS

1. An analysis of losses in the initial parameters of solar cells based on CdS/CdTe showed that in order to increase the efficiency of the device structure, it is necessary to reduce the recombination rate of minority charge carriers in the volume of the photovoltaic converter, reduce the series resistance and conductivity of the shunt level.

The main directions for increasing the efficiency of CdS/CdTe based SCs by increasing  $V_{nl}$  and  $J_{sc}$  have already been implemented, but insufficient attention is paid to increasing the efficiency by increasing the  $FF$  of the light CVC by reducing the series resistance when creating low-tilt rear contacts.

It has been experimentally established that in the absence of a copper interlayer on the rear surface or the absence of an annealing process after the formation of a rear contact, the efficiency of ITO/CdS/CdTe/Cu/Au film SCs is limited at the level of 3–4 %, which is due to the operation of the device structure in the "through diode" mode. When a Cu/Au tunnel contact is formed, the SC efficiency increases to 10 %.

2. The study of transparent Cu/ITO rear contacts for CdTe-based solar cells intended for use in tandem and bilaterally sensitive device structures made it possible to establish that the preliminary deposition of a nanosized copper layer on the CdTe surface to form the back electrode makes it possible to form a high-quality tunnel contact. After 8 years of operation, the efficiency of the studied solar cells practically coincides with the initial one.

It has been established that changing the direction of illumination of the SnO<sub>2</sub>:F/CdS/CdTe/Cu/ITO SCs leads to a significant decrease in the efficiency of the device structure. The differences in the initial parameters and light diode characteristics of SnO<sub>2</sub>:F/CdS/CdTe/Cu/ITO SCs are due to the effect of the rear diode on the efficiency of photovoltaic processes in the base layer.

3. Using the DC magnetron sputtering method, experimental samples of a module based on cadmium telluride on a flexible polyamide substrate have been obtained, consisting of four micro-modules with series-connected solar cells. Researches of initial parameters and light diode characteristics of the micromodules which are a part of the module have been carried out.

It has been found that the maximum efficiency of the micromodule as part of the module reached 5.3 %. It has been established that the low efficiency values of micromodules are due to the partial shunting of solar cells in the composition of micromodules and inefficient absorption of the visible part of the radiation when passing through the polyamide substrate.

## CONFLICT OF INTEREST

The authors declare that they have no conflict of interest in relation to this research, whether financial, personal, authorship or otherwise, that could affect the research and its results presented in this paper.

## REFERENCES

1. Rashkevich, N., Shevchenko, R., Khmyrov, I., Soshinskiy, A. (2021). Investigation of the Influence of the Physical Properties of Landfill Soils on the Stability of Slopes in the Context of Solving Civil Security Problems. *Materials Science Forum*, 1038, 407–416. doi: <https://doi.org/10.4028/www.scientific.net/msf.1038.407>
2. Yeremenko, S., Sydorenko, V., Andrii, P., Shevchenko, R., Vlasenko, Y. (2021). Existing Risks of Forest Fires in Radiation Contaminated Areas: A Critical Review. *Ecological Questions*, 32 (3), 35–47. doi: <https://doi.org/10.12775/eq.2021.022>
3. Gurbanova, M., Loboichenko, V., Leonova, N., Strelets, V., Shevchenko, R. (2020). Comparative assessment of the ecological characteristics of auxiliary organic compounds in the composition of foaming agents used for fire fighting. *Bulletin of the Georgian National Academy of Sciences*, 14 (4), 58–66.
4. Kirichenko, M. V., Zaitsev, R. V., Deyneko, N. V., Kopach, V. R., Antonova, V. A., Listratenko, A. M. (2008). Influence of Constructive and Technological Solutions of Silicon Solar Cells on Minority Carrier Parameters of Base Crystals. *Telecommunications and Radio Engineering*, 67 (3), 227–240. doi: <https://doi.org/10.1615/telecomradeng.v67.i3.40>
5. Romeo, N., Bosio, A., Romeo, A. (2010). An innovative process suitable to produce high-efficiency CdTe/CdS thin-film modules. *Solar Energy Materials and Solar Cells*, 94 (1), 2–7. doi: <https://doi.org/10.1016/j.solmat.2009.06.001>
6. De Vos, A., Parrott, J., Baruch, P., Landsberg, P. (1994). Bandgap effects in thin-film heterojunction solar cells. *Proceeding 12th European Photovoltaic Solar Energy Conference*. Amsterdam, 1315–1319.
7. 16.5 %-Efficient CdS/CdTe polycrystalline thin-film solar cell (2001). *17th European Photovoltaic Solar Energy Conference*. Munich, 995–1000.
8. Köntges, M., Reineke-Koch, R., Nollet, P., Beier, J., Schäffler, R., Parisi, J. (2002). Light induced changes in the electrical behavior of CdTe and Cu(In,Ga)Se<sub>2</sub> solar cells. *Thin Solid Films*, 403-404, 280–286. doi: [https://doi.org/10.1016/s0040-6090\(01\)01507-3](https://doi.org/10.1016/s0040-6090(01)01507-3)
9. Zeng, G., Zhang, J., Li, B., Li, W., Wu, L., Wang, W., Feng, L. (2015). Effects of different CdCl<sub>2</sub> annealing methods on the performance of CdS/CdTe polycrystalline thin film solar cells. *Science China Technological Sciences*, 58 (5), 876–880. doi: <https://doi.org/10.1007/s11431-015-5787-2>
10. Riech, I., Peña, J. L., Ares, O., Rios-Flores, A., Rejón-Moo, V., Rodríguez-Fragoso, P., Mendoza-Alvarez, J. G. (2012). Effect of annealing time of CdCl<sub>2</sub> vapor treatment on CdTe/CdS interface properties. *Semiconductor Science and Technology*, 27 (4), 045015. doi: <https://doi.org/10.1088/0268-1242/27/4/045015>
11. Khrypunov, G. (2010). Development organic back contact for thin-film CdS/CdTe solar cell. *Physics and Chemistry of Solid State*, 11 (1), 248–251.

12. Wu, H. (2014). p-CdTe/n-CdS photovoltaic cells in the substrate configuration. University of Rochester.
13. Enzenroth, R. A., Barth, K. L., Sampath, W. S. (2005). Correlation of stability to varied CdCl<sub>2</sub> treatment and related defects in CdS/CdTe PV devices as measured by thermal admittance spectroscopy. *Journal of Physics and Chemistry of Solids*, 66 (11), 1883–1886. doi: <https://doi.org/10.1016/j.jpcs.2005.09.022>
14. Bätzner, D. L., Romeo, A., Zogg, H., Wendt, R., Tiwari, A. N. (2001). Development of efficient and stable back contacts on CdTe/CdS solar cells. *Thin Solid Films*, 387 (1-2), 151–154. doi: [https://doi.org/10.1016/s0040-6090\(01\)00792-1](https://doi.org/10.1016/s0040-6090(01)00792-1)
15. Mamazza, R., Balasubramanian, U., More, D. L., Ferekides, C. S. (2002). Thin films of CdIn<sub>2</sub>O<sub>4</sub> as transparent conducting oxides. *Proceeding of the 29nd IEEE Photovoltaic Specialists Conference*. Anaheim, 616–619. doi: <https://doi.org/10.1109/pvsc.2002.1190640>
16. Minami, T., Kakumu, T., Takeda, Y., Takata, S. (1996). Highly transparent and conductive ZnO In<sub>2</sub>O<sub>3</sub> thin films prepared by d.c. magnetron sputtering. *Thin Solid Films*, 290-291, 1–5. doi: [https://doi.org/10.1016/s0040-6090\(96\)09094-3](https://doi.org/10.1016/s0040-6090(96)09094-3)
17. Effect of CdCl<sub>2</sub> treatment on the interior of CdTe crystal (2001). *Proceeding Materials Research Society Symposium*. San Francisco, H1.6.1–H1.6.12.
18. Romeo, A., Bätzner, D. L., Zogg, H., Tiwari, A. N. (2000). Recrystallization in CdTe/CdS. *Thin Solid Films*, 361-362, 420–425. doi: [https://doi.org/10.1016/s0040-6090\(99\)00753-1](https://doi.org/10.1016/s0040-6090(99)00753-1)
19. Sandhu, A., Kobayashi, K., Okamoto, T., Yamada, A., Konagai, M. (2001). Effect of CdCl<sub>2</sub> Treatment Conditions on the Deep Level Density, Carrier Lifetime and Conversion Efficiency of CdTe Thin Film Solar Cells. *MRS Proceedings*. San Francisco, 668, H8.13.1–H8.13.6. doi: <https://doi.org/10.1557/proc-668-h8.13>
20. High-efficiency Cd<sub>2</sub>SnO<sub>4</sub>/Zn<sub>2</sub>SnO<sub>4</sub>/ZnxCd<sub>1-x</sub>S/CdS/CdTe polycrystalline thin-film solar cells (2002). *Proc. 29th IEEE Photovoltaics Specialists Conf*. New Orleans, 470–474.
21. Demtsu, S. H., Sites, J. R. (2005). Quantification of losses in thin-film CdS/CdTe solar cells. *Conference Record of the Thirty-First IEEE Photovoltaic Specialists Conference*, 347–350. doi: <https://doi.org/10.1109/pvsc.2005.1488140>
22. Schottky diode current (2002). *Proc. 29th IEEE Photovoltaics Specialists Conf*. New Orleans, 535–538.
23. Terheggen, M., Heinrich, H., Kostorz, G., Baetzner, D., Romeo, A., Tiwari, A. N. (2004). Analysis of Bulk and Interface Phenomena in CdTe/CdS Thin-Film Solar Cells. *Interface Science*, 12 (2/3), 259–266. doi: <https://doi.org/10.1023/b:ints.0000028655.11608.c7>
24. Green, M. A. (1992). *Solar cells: operating principles, technology and system applications*. University of New South Wales. Kensington, 274.
25. Khrypunov, G., Meriuts, A., Klyui, N., Shelest, T., Deyneko, N., Kovtun, N. (2010). Development of back contact for CdS/CdTe thin-film solar cells. *Functional materials*, 17 (1), 114–119.

26. Bätzner, D. L., Wendt, R., Romeo, A., Zogg, H., Tiwari, A. N. (2000). A study of the back contacts on CdTe/CdS solar cells. *Thin Solid Films*, 361-362, 463–467. doi: [https://doi.org/10.1016/s0040-6090\(99\)00842-1](https://doi.org/10.1016/s0040-6090(99)00842-1)
27. Meriuts, A. V., Khrypunov, G. S., Shelest, T. N., Deyneko, N. V. (2010). Features of the light current-voltage characteristics of bifacial solar cells based on thin CdTe layers. *Semiconductors*, 44 (6), 801–804. doi: <https://doi.org/10.1134/s1063782610060187>
28. Research, Solar Cell Production and Market Implementation of Photovoltaics (2004). European Commission, DG JRC, Institute for Environment and Sustainability Energies Unit Via Enrico Fermi 1; TP 450 I – 21020. Ispra, 95.
29. Mitchell, K., Fahrenbruch, A. L., Bube, R. H. (1977). Photovoltaic determination of optical-absorption coefficient in CdTe. *Journal of Applied Physics*, 48 (2), 829–830. doi: <https://doi.org/10.1063/1.323636>
30. Khrypunov, G. S., Sokol, E. I., Iakimenko, Iu. I., Meriutc, A. V., Ivashchuk, A. V., Shelest, T. N. (2014). Conversion of solar energy by combination solar cells based on CdTe and CuInSe<sub>2</sub>. *Fizika i tehnika poluprovodnikov*, 48 (12), 1671–1675.
31. Jackson, P., Hariskos, D., Lotter, E., Paetel, S., Wuerz, R., Menner, R., Wischmann, W., Powalla, M. (2011). New world record efficiency for Cu(In,Ga)Se<sub>2</sub> thin-film solar cells beyond 20 %. *Progress in Photovoltaics: Research and Applications*, 19 (7), 894–897. doi: <https://doi.org/10.1002/pip.1078>
32. Khrypunov, G., Vambol, S., Deyneko, N., Sychikova, Y. (2016). Increasing the efficiency of film solar cells based on cadmium telluride. *Eastern-European Journal of Enterprise Technologies*, 6 (5 (84)), 12–18. doi: <https://doi.org/10.15587/1729-4061.2016.85617>
33. Li, J., Zhang, Y., Gao, T., Hu, C., Yao, T., Yuan, Q. et al. (2017). Quantum dot-induced improved performance of cadmium telluride (CdTe) solar cells without a Cu buffer layer. *Journal of Materials Chemistry A*, 5 (10), 4904–4911. doi: <https://doi.org/10.1039/c6ta10441j>
34. Deyneko, N., Khrypunov, G., Semkiv, O. (2018). Photoelectric Processes in Thin-film Solar Cells Based on CdS/CdTe with Organic Back Contact. *Journal of Nano- and Electronic Physics*, 10 (2), 02029-1–02029-4. doi: [https://doi.org/10.21272/jnep.10\(2\).02029](https://doi.org/10.21272/jnep.10(2).02029)
35. Alonzo, J., Kochemba, W. M., Pickel, D. L., Ramanathan, M., Sun, Z., Li, D. et al. (2013). Assembly and organization of poly(3-hexylthiophene) brushes and their potential use as novel anode buffer layers for organic photovoltaics. *Nanoscale*, 5 (19), 9357–9364. doi: <https://doi.org/10.1039/c3nr02226a>
36. Burmenko, A., Deyneko, N., Hrebtsova, I., Kryvulkin, I., Prokopenko, O., Shevchenko, R., Tarasenko, O. (2020). Investigating an alternative electricity supply system for preventing emergencies under conditions of limited capacity. *Eastern-European Journal of Enterprise Technologies*, 3 (12 (105)), 56–61. doi: <https://doi.org/10.15587/1729-4061.2020.206395>

37. Deyneko, N., Zhuravel, A., Mikhailova, L., Naden, E., Onyshchenko, A., Savchenko, A., Strelets, V., Yurevych, Y. (2020). Devising a technique to improve the efficiency of CdS/CdTe/Cu/Au solar cells intended for use as a backup power source for the systems of safety and control of objects. *Eastern-European Journal of Enterprise Technologies*, 6 (5 (108)), 21–27. doi: <https://doi.org/10.15587/1729-4061.2020.220489>
38. Deyneko, N., Yeremenko, S., Kamyshentsev, G., Kryvulkin, I., Matiushenko, M., Myroshnyk, O. et al. (2021). Development of a method for obtaining a CdS/CdTe/Cu/Au module on a flexible substrate designed for backup supplying systems prevention of emergency situations. *Eastern-European Journal of Enterprise Technologies*, 1 (5 (109)), 31–36. doi: <https://doi.org/10.15587/1729-4061.2021.225694>
39. Venkatesan, M., McGee, S., Mitra, U. (1989). Indium tin oxide thin films for metallization in microelectronic devices. *Thin Solid Films*, 170 (2), 151–162. doi: [https://doi.org/10.1016/0040-6090\(89\)90719-0](https://doi.org/10.1016/0040-6090(89)90719-0)
40. Jeong, W.-J., Park, G.-C. (2001). Electrical and optical properties of ZnO thin film as a function of deposition parameters. *Solar Energy Materials and Solar Cells*, 65 (1-4), 37–45. doi: [https://doi.org/10.1016/s0927-0248\(00\)00075-1](https://doi.org/10.1016/s0927-0248(00)00075-1)
41. Deyneko, N., Semkiv, O., Khmyrov, I., Khryapynskyy, A. (2018). Investigation of the combination of ITO/CdS/CdTe/Cu/Au solar cells in microassembly for electrical supply of field cables. *Eastern-European Journal of Enterprise Technologies*, 1 (12 (911)), 18–23. doi: <https://doi.org/10.15587/1729-4061.2018.124575>
42. Chernykh, E. P., Khripunov, G. C., Boiko, B. T. (2002). Otcenka stekhiometrii absorbernykh sloev CuGaSe<sub>2</sub> i CuIn<sub>0,7</sub>Ga<sub>0,3</sub>Se<sub>2</sub> plenochnykh fotoelektricheskikh preobrazovatelei. *Visnik Sumskogo derzhavnogo universitetu*, 13 (46), 133–140.
43. Boyko, B., Khrypunov, G., Kharchenko, M., Chernikov, A. (2001). Examination of thermal stability of ZnO:Al films obtained by RF-magnetron sputtering without preheating of substrate. *Proceeding of 17th European Photovoltaic Solar Energy Conversion and Exhibition. Munich*, 1128–1130.
44. Boiko, B. T., Chernykh, O. P., Khrypunov, H. S., Kopach, H. Y. (2001). Plivkovi fotoelektrychni peretvorivuvachi na osnovi CuGaSe<sub>2</sub>. *Fizyka i khimiiia tverdogo tila*, 2 (4), 549–558.
45. Khrypunov, G. S., Kopach, V. R., Meriuts, A. V., Zaitsev, R. V., Kirichenko, M. V., Deyneko, N. V. (2011). The influence of prolonged storage and forward-polarity voltage on the efficiency of CdS/CdTe-based film solar cells. *Semiconductors*, 45 (11), 1505–1511. doi: <https://doi.org/10.1134/s1063782611110133>
46. Bolbas, O., Deyneko, N., Yeremenko, S., Kyrillova, O., Myrgorod, O., Soshinsky, O. et al. (2019). Degradation of CdTe SC during operation: modeling and experiment. *Eastern-European Journal of Enterprise Technologies*, 6 (12 (102)), 46–51. doi: <https://doi.org/10.15587/1729-4061.2019.185628>
47. Vambol, S., Vambol, V., Sychikova, Y., Deyneko, N. (2017). Analysis of the ways to provide ecological safety for the products of nanotechnologies throughout their life cycle.

- Eastern-European Journal of Enterprise Technologies, 1 (10 (85)), 27–36. doi: <https://doi.org/10.15587/1729-4061.2017.85847>
48. Romeo, A., Bätzner, D. L., Zogg, H., Tiwari, A. N. (2001). Influence of proton irradiation and development of flexible CdTe solar cells on polyimide. MRS Proceedings. San Francisco, 668, H3.3.1–H3.3.6. doi: <https://doi.org/10.1557/proc-668-h3.3>
  49. Batzner, D. L., Romeo, A., Zogg, H., Tiwari, A. N., Wendt, R. (2003). Effect of back contact metallization on the stability of CdTe/CdS solar cells. 16 European Photovoltaic Solar Energy Conference: Proceeding of the conference. Glasgow, 353–356.
  50. Leterrier, Y., Médico, L., Demarco, F., Manson, J.-A. E., Betz, U., Escolà, M. F. et al. (2004). Mechanical integrity of transparent conductive oxide films for flexible polymer-based displays. Thin Solid Films, 460 (1-2), 156–166. doi: <https://doi.org/10.1016/j.tsf.2004.01.052>
  51. Leterrier, Y., Pinyol, A., Gilliéron, D., Manson, J.-A. E., Timmermans, P. H. M., Bouten, P. C. P. et al. (2010). Mechanical failure analysis of thin film transistor devices on steel and polyimide substrates for flexible display applications. Engineering Fracture Mechanics, 77 (4), 660–670. doi: <https://doi.org/10.1016/j.engfracmech.2009.12.016>
  52. Borysenko, I., Burmenko, O., Deyneko, N., Zobenko, O., Yivzhenko, Y., Kamyshentsev, G. et al. (2021). Development of a method for producing effective CdS/CdTe/Cu/Au solar elements on a flexible substrate designed for backup supplying systems prevention of emergency situations. Eastern-European Journal of Enterprise Technologies, 6 (5 (114)), 6–11. doi: <https://doi.org/10.15587/1729-4061.2021.247720>
  53. McCandless, B. E. (2001). Thermochemical and Kinetic Aspects of Cadmium Telluride Solar Cell Processing. MRS Proceedings, 668, H1.6.1–H1.6.10. doi: <https://doi.org/10.1557/proc-668-h1.6>
  54. Deyneko, N., Semkiv, O., Soshinsky, O., Strelets, V., Shevchenko, R. (2018). Results of studying the Cu/ITO transparent back contacts for solar cells SnO<sub>2</sub>:F/CdS/CdTe/Cu/ITO. Eastern-European Journal of Enterprise Technologies, 4 (5 (94)), 29–34. doi: <https://doi.org/10.15587/1729-4061.2018.139867>
  55. Izu, M., Ellison, T. (2003). Roll-to-roll manufacturing of amorphous silicon alloy solar cells with in situ cell performance diagnostics. Solar Energy Materials and Solar Cells, 78 (1-4), 613–626. doi: [https://doi.org/10.1016/s0927-0248\(02\)00454-3](https://doi.org/10.1016/s0927-0248(02)00454-3)
  56. Deyneko, N., Kovalev, P., Semkiv, O., Khmyrov, I., Shevchenko, R. (2019). Development of a technique for restoring the efficiency of film ITO/CdS/CdTe/Cu/Au SCs after degradation. Eastern-European Journal of Enterprise Technologies, 1 (5 (97)), 6–12. doi: <https://doi.org/10.15587/1729-4061.2019.156565>
  57. Söderström, K., Escarré, J., Cubero, O., Haug, F.-J., Perregaux, S., Ballif, C. (2010). UV-nano-imprint lithography technique for the replication of back reflectors for n-i-p thin film silicon solar cells. Progress in Photovoltaics: Research and Applications, 19 (2), 202–210. doi: <https://doi.org/10.1002/pip.1003>
-

58. Deyneko, N., Kryvulkin, I., Matiushenko, M., Tarasenko, O., Khmyrov, I., Khmyrova, A., Shevchenko, R. (2019). Investigation of photoelectric converters with a base cadmium telluride layer with a decrease in its thickness for tandem and two-sided sensitive instrument structures. *EUREKA: Physics and Engineering*, 5, 73–80. doi: <https://doi.org/10.21303/2461-4262.2019.001002>
59. Deyneko, N. (2020). Study of Methods for Producing Flexible Solar Cells for Energy Supply of Emergency Source Control. *Materials Science Forum*, 1006, 267–272. doi: <https://doi.org/10.4028/www.scientific.net/msf.1006.267>
60. First Solar sets world record for CdTe solar cell efficiency (2014). Solar First. Available at: <https://investor.firstsolar.com/news/press-release-details/2014/First-Solar-Sets-World-Record-for-CdTe-Solar-Cell-Efficiency/default.aspx>